Mira Geoscience Limited
310 Victoria Ave, Suite 309
Westmount, QC
Canada H3Z 2M9

Tel: (514) 489-1890
Fax: (514) 489-5536
info@miragеoscience.com
www.miragеoscience.com

Exploration Targeting at the Buenaventura Project, Chile

Final Report Prepared for:

Minera Tierra Noble

November 2011

Mira Geoscience
...modelling the earth

1 Introduction

The objective of the Tierra Noble Buenaventura exploration targeting project is to identify zones within the Buenaventura project area that have the potential to host Fe-oxide Cu-Au mineralization. A 3D Common Earth Model (CEM) was built from compiled geological, geochemical, and geophysical data in combination with magnetic, gravity, and ZTEM 3D inversion models calculated from geophysical data collected over the Buenaventura property. The Gocad Targeting Workflow was applied to the CEM. Targeting was carried out using a knowledge-based approach where experts decide upon relevant exploration criteria, and associated cut-offs and weights for balancing criteria against one another.

The final model will be adaptable to further targeting studies. This can be accomplished by updating the exploration criteria embodied within the 3D model to reflect new exploration concepts or new data as it becomes available. The framework for furthering exploration targeting models and concepts is now in place.

1.1 Targeting Methodology

The targeting methods employed here are inspired by a history of successful application in 2D GIS systems in mineral exploration going back to the 1980's and 1990's (see for example Bonham-Carter, 1994 and 1997), and more recent experimentation in 3D for exploration applications (Apel and Böhme, 2006; Caumon et al., 2006).

With any exploration targeting project, computer-aided or not, the first step is to define the characteristics of the target. Establishment of exploration criteria can be carried out from standard ore deposit models, which provide general information, or derived from site-specific geological knowledge. With either approach, the postulated criteria are modelled in 3D to the best extent possible given the data in hand.

A Gocad multi-disciplinary Common Earth Model (CEM) is created as the fundamental data support for the various types of data that are to serve as the exploration criteria. The exploration criteria are modelled as quantitative or classified properties in a 3D block model encompassing

the exploration volume. Exploration criteria are typically a mixture of interpreted rock properties such as lithology, geochemistry, and physical properties, and non-rock property target indicators such as depth, and proximity to faults or significant contacts. “Target” locations are identified, ranked, and classified by computing and analyzing a score at each cell of the 3D grid. The process is summarized graphically in Figure 1.

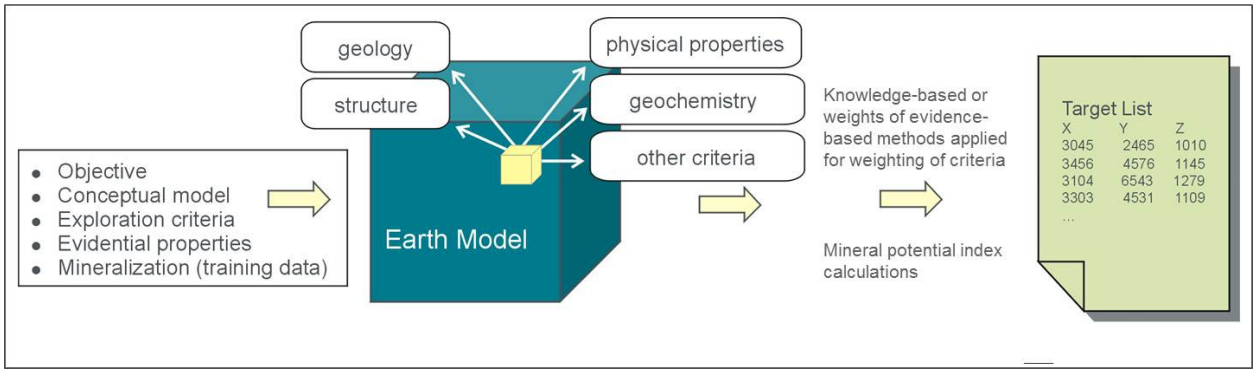

Figure 1. Project flow for generating exploration targets.

Criteria used to generate the mineral potential model can be combined in various ways to explore the influence of different datasets on the results. Anomalies that consistently occur between workflow results may be considered most robust.

In this project we are considering only criteria that relate to IOCG style targets. Other mineralization types may be represented in the project area and, while not explicitly included in this study, the final 3D Common Earth Model provides a solid foundation with which to commence targeting such non-IOCG mineralization styles.

1.2 Geological Background

Tierra Noble’s Buenaventura property lies within the Atacama Desert approximately 50 km north-northeast from the town of Copiapo, Chile. Mineralization found on the property has characteristics similar to some of the Chilean Fe-oxide copper gold (IOCG) deposits that occur

and are mined regionally. Two globally significant Cu producers are IOCG deposits Candelaria, and Mantoverde (Figure 2). The Buenaventura property sits in favorable location along the > 1000 km long north-south trending crustal scale Atacama Fault Zone, a structure believed to play a role in the localization of Candelaria, Mantoverde and numerous other Fe-oxide and IOCG deposits in Chile.

Figure 2. IOCG deposits of Chile (www.marianaresources.com).

Mira Geoscience
...modelling the earth

Geology

The geology on the Buenaventura property (Figure 3) is dominated by the andesitic volcanic and volcaniclastic rocks of the late Jurassic to early Cretaceous Punta del Cobre formation (on regional maps, dipping shallowly northeast). Several zones of hydrothermal and tectonic breccia hosted by Punta del Cobre volcanic rocks, have been mapped in drillcore, as well as in outcrop at Cerro Breccia and at Cerro Amada (Figure 3). Hydrothermal-magmatic breccias are a common feature in many IOCG deposits, often acting as a host for mineralization.

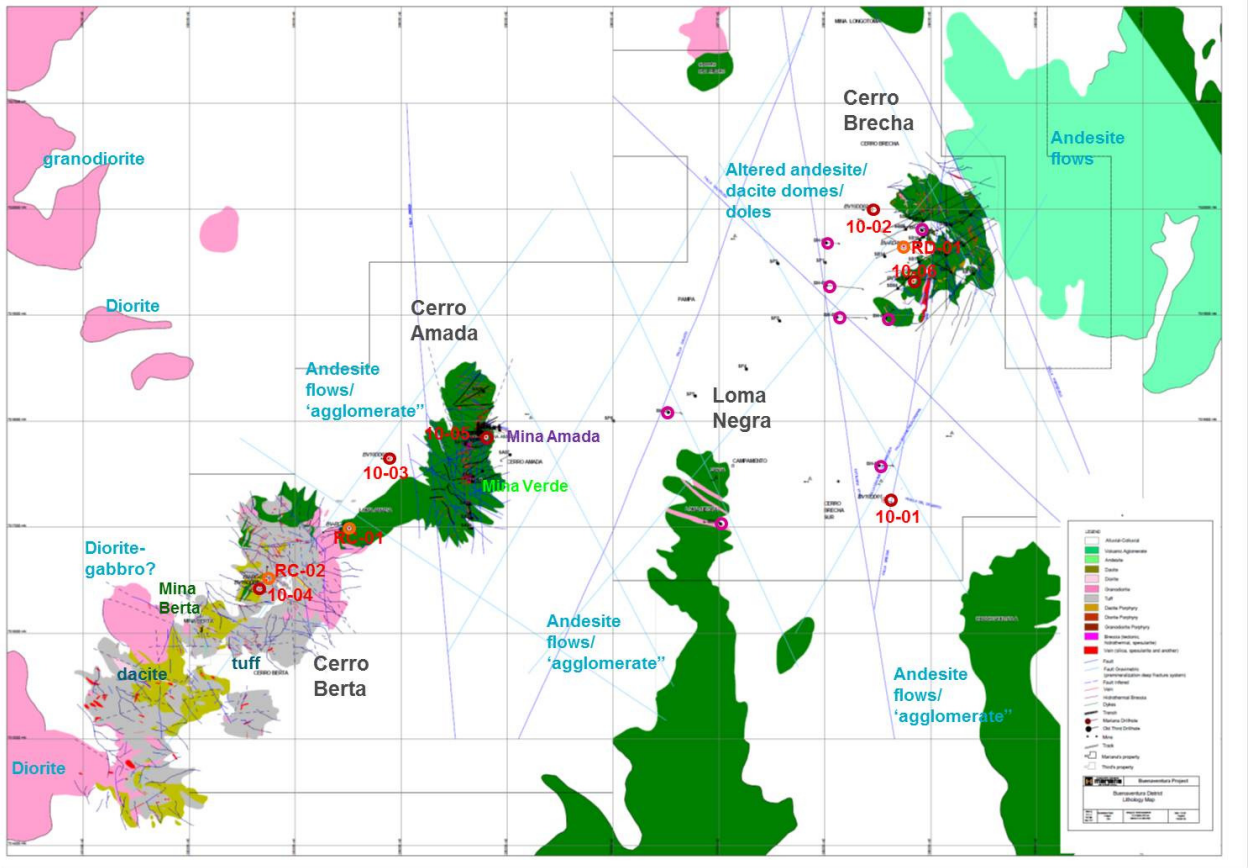

Figure 3. Geology of the Buenaventura property.

Punta del Cobre rocks are mapped to be in faulted contact with massive coherent andesitic flows of the slightly older middle to late Jurassic La Negra formation in the northwestern corner of the property.

The western edge of the property encompasses the eastern margin of the San Juan pluton. Although granodiorite is the dominant phase at the district scale, near the Buenaventura property boundary, additional intrusive phases occur including clinopyroxene diorite.

At the southwestern corner of the property some dacitic and tuffaceous units have been mapped. From drillcore, these units sit above deeper intrusive granodioritic rocks.

The Chivato Fault, an extensive regional scale fault displaying sinistral movement trends northeast-southwest across the Quebrada Salitrosa regional geological map. The fault is projected to cross-cut Buenaventura property geology, however it is not explicitly mapped on the property. From magnetics data and magnetic inversion modelling, a strongly magnetic feature runs through the property, parallel to the projected Chivato Fault. The feature is interpreted as being a buried elongate intrusive body, as it appears to align with intrusive rocks to the south recorded on the Copiapo regional geological map. Based on inversion results however, this feature is of significantly high susceptibility, with values modelled that would normally reflect rocks with significant magnetite content.

Although geological contacts and magnetic features suggest a local, dominantly northeast structural trend, several mapped and interpreted faults trend northwest (Figure 3). These northwest-trending features are of particular interest as this is the orientation of Atacama Fault Zone splays localizing the Candelaria deposit to the south and the Mantoverde deposit to the north.

Alluvial and fluvial deposits cover a significant area of the Buenaventura property. Within the district these Miocene to Quaternary deposits are recorded to be as deep as at least 300m.

Sulfide mineralization and Fe-oxides are recorded at various locations throughout the Buenaventura property, with the most significant mineralization to date found in the Cerro Breccia and Cerro Amada areas. Some small past producing workings occur within the property

bounds including Mina Berta (tenement not controlled by Tierra Noble), Mina Amada, and Mina Verde, in addition to some other smaller Cu mineralized sites.

Alteration

Alteration does not seem to follow a clear pattern at Buenaventura. Hydrolytic alteration has been mapped pervasively within andesitic volcanic units across the property (Figure 4). Sodic alteration occurs in the west, near Cerro Berta and Cerro Amada. Silicification is recorded at the Mina Berta mine. Some small zones of potassic alteration are known. Hydrolytic alteration is common to the upper portions of IOCG systems, while potassic alteration is often indicative of the core of magmatic hydrothermal alteration systems. Sodic and sodic-calcic alteration tends to be more regional in nature.

1.3 Deposit Model and Exploration Strategy

To guide exploration, deposit models for IOCG deposits in general, but specifically nearby Candelaria and Mantoverde, are considered. These deposits provide examples of typical IOCG metal and alteration signatures, as well as provide insight into typical dimensions of magmatic-hydrothermal and mineralized systems.

The following notes are derived principally from the Cliffs Natural Resources IOCG Workshop held in Vancouver, January 28-30, 2011, which presented a wide survey of IOCG deposits and exploration strategies. We will focus on aspects of the conceptual model that can be translated into observable, quantifiable exploration criteria that will ultimately be represented as queryable entities in the 3D targeting model. From Hitzman (2011) the general characteristics of a *sensu stricto* IOCG deposit are the following:

- commonly associated with pre-sulphide sodic or sodic-calcic alteration on a large, often regional, scale relative to economic mineralization;
- most IOCG ore is associated with potassic, calcic, or hydrolytic alteration assemblages;

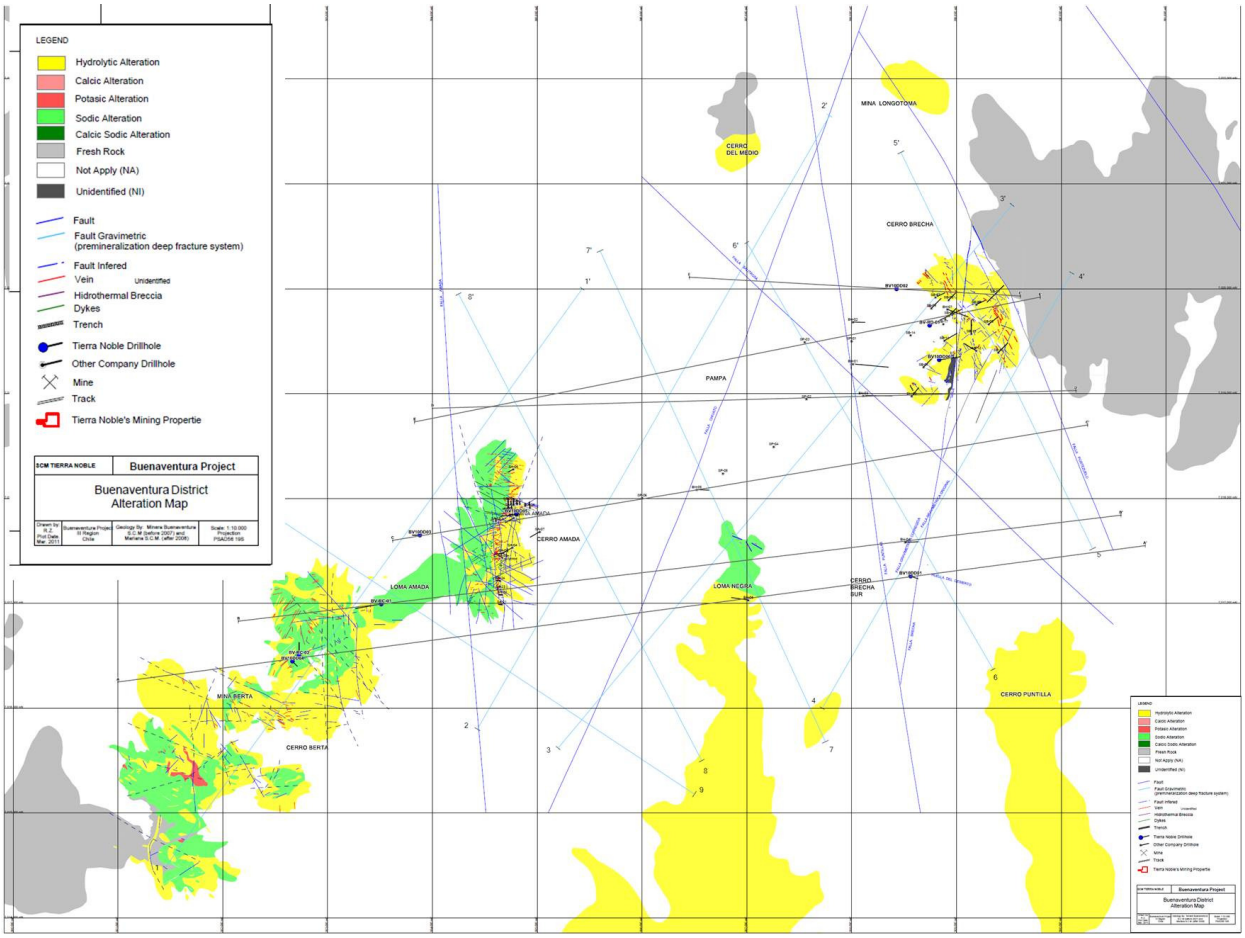

Figure 4. Alteration mapped at Buenaventura.

- highly variable deposit morphology;
- structurally controlled (associated with high- or low-angle faults that are commonly splays off crustal features) and commonly contain significant volumes of breccia;
- deposit mineralogy: iron oxide minerals (magnetite, hematite) dominant, minor sulphides (generally chalcopyrite, lesser pyrite), gangue feldspar, mica, calc-silicate minerals, carbonates, barite, quartz;

- trace element signature highly variable, reflecting the geochemistry of the crust that the hydrothermal fluids are moving through (Candelaria associated with Zn, Co, Ag);
- alteration minerals change with protolith and depth or distance from the hydrothermal fluid conduit;
- have abundant low-Ti iron oxides and/or iron silicates intimately associated with, but generally earlier than, Fe-Cu sulphides;
- have low-S sulphides (lack of abundant pyrite);
- generally have elevated (anomalous) Ce and La;
- lack significant or abundant quartz veins or silicification;
- show a clear temporal, but not close spatial, relationship to major magmatic intrusions;
- form from highly oxidized, saline fluids.

A schematic cross section of the Candelaria deposit example is depicted in Figure 5.

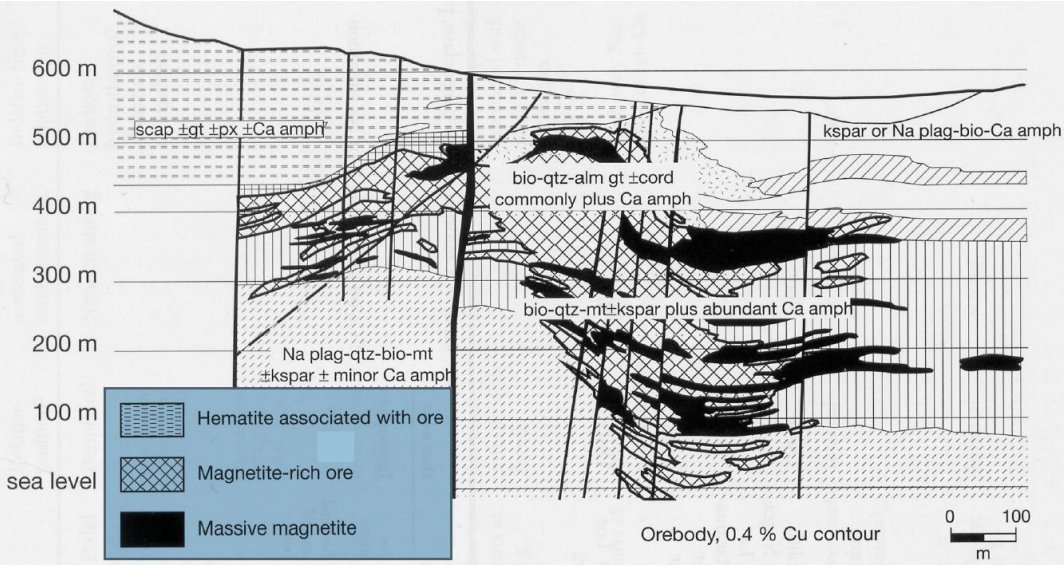

Figure 5. Detailed schematic cross section of the Candelaria deposit indicating major mineralization groups (Marschik and Fonboté, 2001).

The following are specific characteristics of the Candelaria deposit that may be translated into observable exploration criteria:

- hematite body at the top of the sequence and/or deep magnetite body low in the sequence;
- presence of plumbing system (AFZ – *Atacama Fault* Zone – offset feature);
- alteration associated with the system:
    - proximal potassic (potassium feldspar, biotite)
    - distal calcic (actinolite, carbonate, epidote)
    - distal sodic (albite)
    - Cu/Au ~10,000
    - multiple phase alteration process
    - change of oxidation stage
- hydrothermal breccia, volcanics, intrusives
- density ~ 3 g/cm^{-3}.

1.4 Data Available for 3D Modelling and Targeting

The small past-producing workings on the Buenaventura property have predominantly been mined for Cu, however the different showings appear to exhibit variations in mineral distribution and in related alteration assemblages. As such they do not necessarily give a consistent indication of the type of mineralization to be expected elsewhere on the property. To thoroughly investigate the property for the ranges of mineralization and alteration that might occur, and to better understand geology below the extensive overburden, many different geochemical and geophysical methods and tools have been applied.

The data provided to Mira Geoscience for this project include:

- Topography (combined contoured, ZTEM, and SRTM topography)

- Property scale geology and alteration maps
- Regional scale geology maps –Quebrada Salitrosa, Copiapo (Servicio Nacional de Geologia y Mineria de Chile)
- Drilling
- Downhole geochemistry
- Downhole mineralogy
- MMI geochemistry
- Ground gravity (Maping Ltda., 2004, and Zonge Ingenieria y Geofisica, 2008)
- Ground magnetics (Maping Ltda.)
- Airborne magnetics (Geotech)
- Airborne ZTEM (Geotech)

The amount of geophysical and geochemical data collected makes the property suitable for a 3D modelling and targeting. Such a project would not only provide subsurface information which could help geological interpretations, but also aid exploration in an area where alteration and mineralization patterns have been difficult to interpret based only on near-surface geological work.

2 3D Common Earth Modelling

2.1 Model Space and Data Compilation

One of the first, crucial steps to be undertaken when building a Common Earth Model (CEM) is to define the extents, depth, scale and resolution of the model. In Gocad, this is typically a voxet object, which is a regular 3D-grid with constant cell sizes. The voxet cells are not required to be equal lengths along each (U, V and W) axis, allowing for flexibility when designing the model scale and resolution. Vertical or horizontal cells can be thinner to better resolve the smallest model details.

The extents of the Buenaventura CEM volume is based roughly on the extents of geophysical data available. The project bounds were designed to run east-west from 379500 m to 392025 m E, north-south from 7013000 m to 7023525 m N, and from 1750 m to -1000 m elevation. This resulted in a 12.5 km × 10.5 km × 2.7 km block model encompassing a volume of approximately 354 km^3. The voxet was then discretized into 25 m × 25 m × 25 m cells producing a total of over 23.4 million cells.

The CEM voxet was modified for the various inversions to match data spacing. The inversion mesh parameters are discussed in the relevant sections. For targeting, the inversion results were projected back onto the 25 × 25 × 25 m voxet.

The coordinate system used is PSAD 56, Zone 19S. All data were either in this coordinate system or converted to this system prior to import into Gocad.

2.2 Topographic surface

Topographic data was available from various sources. Topography datasets were merged to cover an area required by the inversion modelling (maximum area up to 80 km^2 for ZTEM inversions), maintaining high resolution contoured data at the core.

Four datasets were used: 1) 2 m contour data supplied by the client, 2) 5 m contour data supplied by client, 3) SRTM supplied by the client, 35 km^2 extent), and 4) SRTM data downloaded by Mira Geoscience from Dapple (Geosoft) and translated into PSAD56 Z19S (from 35 km^2 extent zone outward to ~80 km^2 extent).

Datasets 1 and 2 were merged, with duplicate data removed. Datasets 3 and 4 were initially regridded at 25 m and merged. It was necessary to later decimate the combined SRTM data to reduce the number of data (reduce file size). A hole was cut in the merged SRTM datasets and the contour data was dropped in. Merged SRTM data was dropped down 5 m to smooth edges.

3 Inversion Modelling Stage 1

During the first stage of modelling for the Buenaventura targeting project, the VPmg gravity inversion code was used to calculate a depth to basement model, and University of British Columbia – Geophysical Inversion Facility (UBC-GIF) inversion codes were used to carry out minimally constrained inversions of magnetic, gravity, and ZTEM data. Reports from the related geophysical surveys are available to the client. For information pertaining to the preprocessing of geophysical datasets used in inversion, and details on inversion specifications, please refer to the relevant sections below.

3.1 Depth to Basement Modelling Using VPmg

The first modelling task was development of a model of the overburden. This model becomes important for constraining near surface cells during magnetic, gravity and EM inversions where a distinct difference is known or expected between the physical properties of the overburden and the underlying bedrock. Constraining near surface inversion model cells can significantly improve the inversion result, with the cells at depth being more effectively estimated.

Depth to bedrock was calculated using VPmg gravity inversion codes. The following summarizes the modelling process.

- Gravity data were gathered over several field seasons over the property at two different station spacings, 100 m and 400 m. The combined data were regridded to 100 m for input into the VPmg program. Free air data were used for VPmg modelling.
- Outcrops mapped by the client, drillhole logs, property and regional scale geological maps, and field observations were available to create an approximation of the top of the basement for the VPmg starting model. The starting surface was additionally manually warped to mimic the trend and expected greater overburden depths along the northwest trending paleo-valley apparent on the regional Quebrada Salitrosa map.
- For VPmg thickness modelling, the process involved alternating between heterogeneous and geometric inversions. Heterogeneous inversion models the expected heterogeneous densities

in the basement rocks while geometric inversion works to modify the starting surface by warping as necessary to fit the observed gravity data, while honoring the estimated low densities of the overburden, as well as the drillhole and outcrop pin points. At Buenaventura the overburden consists of poorly consolidated materials (alluvium and colluvium) of low density, and was estimated to be ~ 2.2 g/cm^3 for modelling purposes.

There are some limitations in use of this method to calculate overburden thickness. Variability in sedimentary layers comprising the overburden may mean that the density is not consistent throughout. Additionally, there are limited data points available for constraining the overburden-bedrock interface to the north and south of existing drilling on the property.

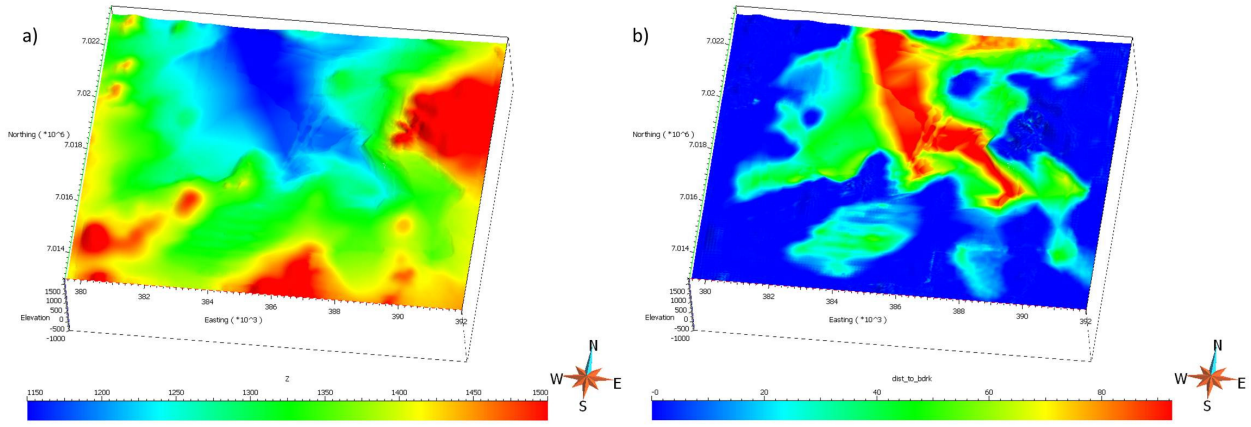

Figure 6. a) Depth of bedrock surface calculated from constrained VPmg modelling, and b) distance to bedrock from topographic surface shown as a property on the depth of bedrock surface.

3.2 Preliminary Geophysical Inversions

3.2.1 Magnetic Inversion

Magnetic data was inverted using UBC-GIF Mag3D inversion codes. Data are shown in Figure 7 and data pre-processing and inversion details are summarized in Table 1. The overburden volume, calculated during VPmg depth to basement modelling, was used as a basic constraint for preliminary magnetic inversions.

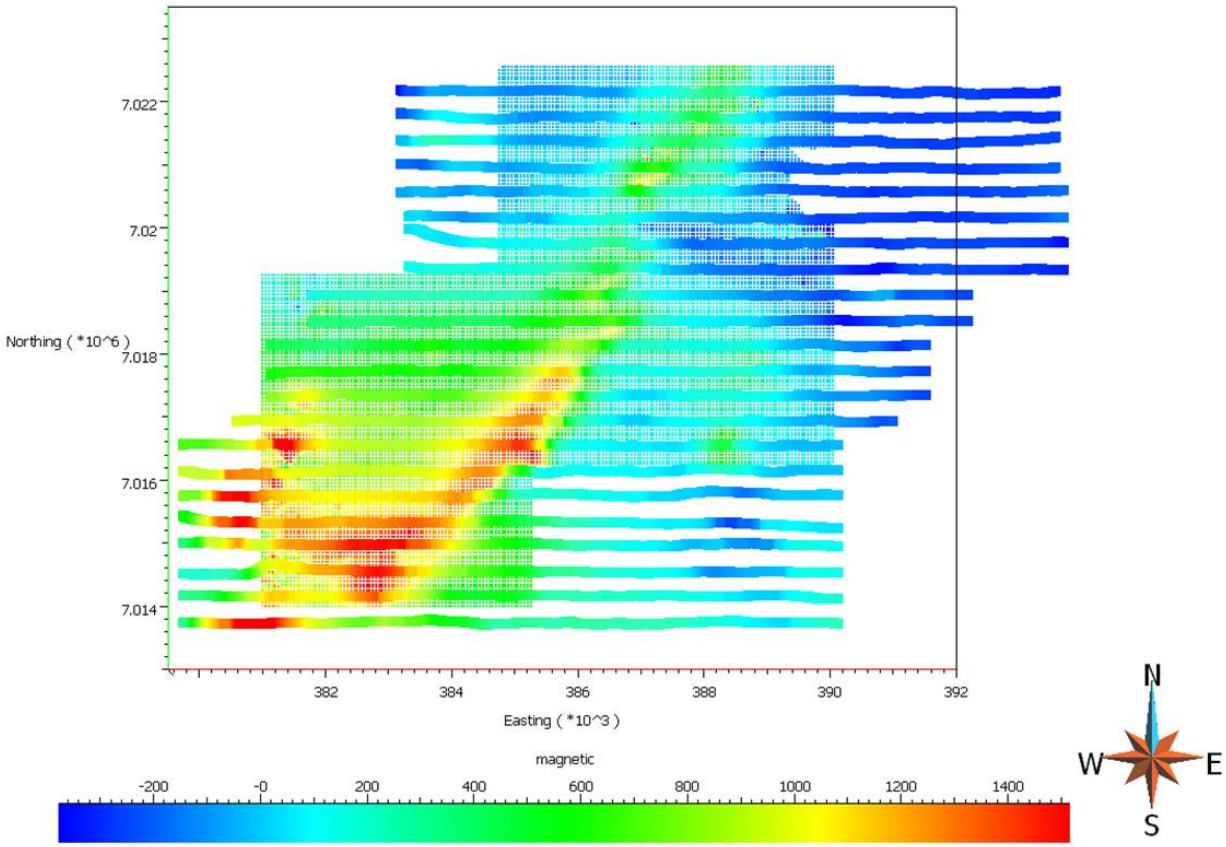

Figure 7. Residual magnetic data from ground surveys, and the ZTEM airborne surveys (nT).

Survey specifications	Ground data	Airborne data
Survey date	March-April 2010	Jan. 8, 2011 - Jan 18, 2011
Sensor	6.2 m above topography	57 m below radar
Diurnally corrected	yes	yes
Latitude	-26.97	-26.96
Longitude	-70.15	-70.14
Line spacing	50	400 m
Receiver spacing	1-4 m	9.5 m
Mean elevation (m)	1440	1440
Magnetic field inclination	-25.5	-25.6
Magnetic field declination	-0.8	-0.95
Magnetic field magnitude (nT)	23493	23442
Inversion pre-processing	Ground data	Airborne data
Downsampling	10	5
Upward continuation	6.3 (half cell size 12.5 minus sensor height 6.2 m)	
Gridded	50 m	50 m
Regional removal	Yes	Yes
Inversion - combined ground and airborne magnetic data sets		
No. data inverted	26383	
Errors	Std dev of 3% of the magnitude with 34 nT floor/minimum value	
Mesh cell sizes	50 x 50 x 25 (Z thickness increases with depth)	
Length scales	150, 150, 150 (Le, Ln, Lz)	
Chifact	0.7	
Achieved misfit	17746	

Table 1. Magnetic data, and survey and inversion specifications.

Figure 8 represents a horizontal slice through the magnetic inversion at 1100 m. Magnetic susceptibility highs appear to correlate with mapped unaltered massive andesitic rocks in the northeast corner of the property, as well as with potentially more intermediate to mafic intrusive phases of the San Juan pluton. A significant northeast trending magnetic body extends across the property along the same strike as the Chivato Fault mapped to the north on regional maps. The magnetic body, which has no surface expression, appears to be offset in several areas perhaps indicating later faulting. Due to spatial correlations with mapped intrusive rocks to the south, and a general dike-like character, this magnetic unit is interpreted to be intrusive. The inversion

indicates this feature dips steeply to the southeast. A strong contrast between susceptibilities related to the central magnetic body and rocks immediately to the west suggests the presence of a significant contact or fault here. Low susceptibility areas are generally correlative with altered andesitic volcanic and volcaniclastic rocks.

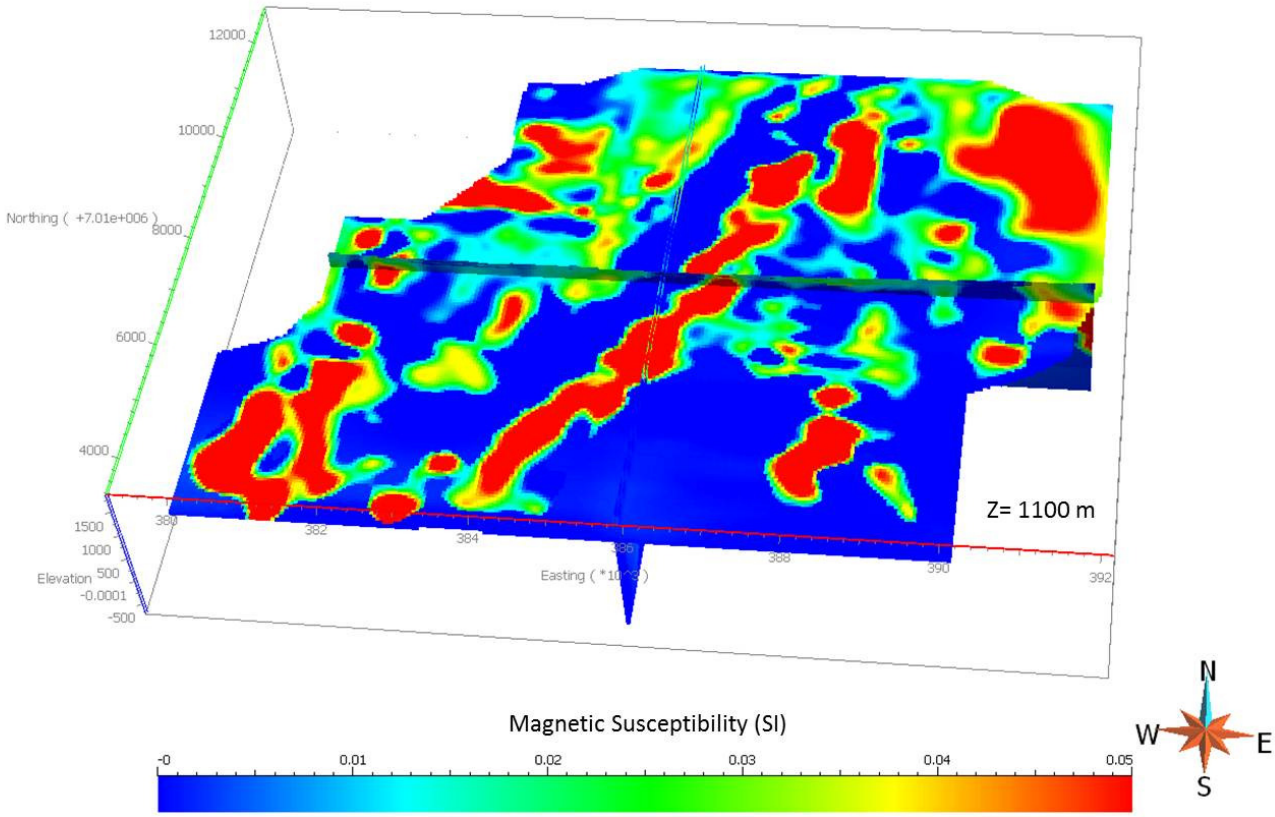

Figure 8. Magnetic inversion result constrained with overburden region.

3.2.2 Gravity Inversion

UBC-GIF 3D gravity inversion codes were used to invert Bouguer corrected (2.4 g/cm^3) ground gravity data from Buenaventura. Data are shown in Figure 9 and data pre-processing and inversion details are summarized in Table 2.

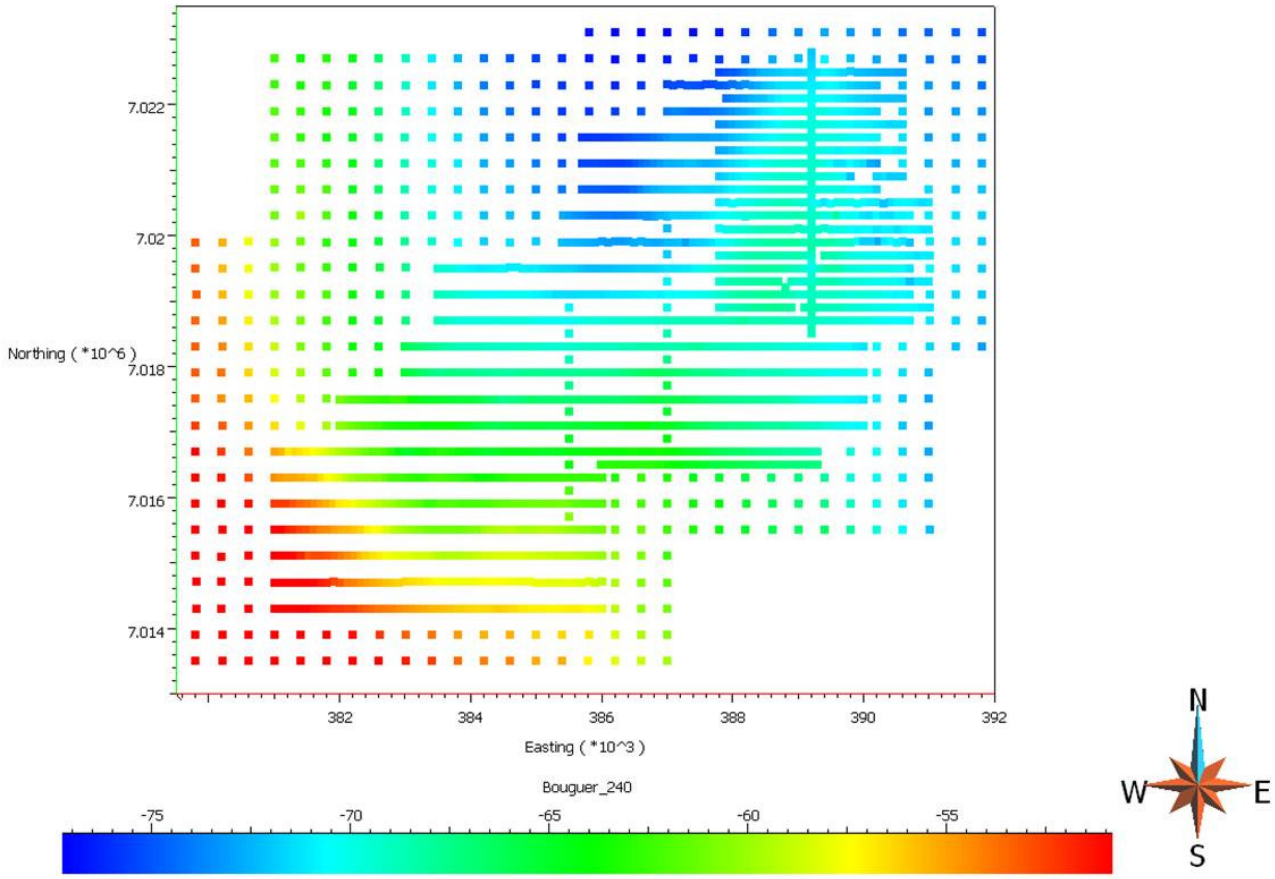

Figure 9. Bouguer corrected ground gravity data (2.4 g/cm^3).

Survey specifications	
Survey dates	2004 and 2008
Sensor height	20 cm
Data elevation	Draped onto topo then lifted 20 cm
Data used	Bouger corrected data (2.6 g/cm^3)
Inversion pre-processing	
Median removed	74 mGal
Gridded	Not gridded
Regional removal	No
Inversion - combined ground and airborne magnetic data sets	
No. data inverted	2018
Errors	Std. dev. of 2% of the magnitude with 1% data range as floor/minimum value
Mesh core cell sizes	50 x 50 x 25
Length scales	150, 150, 75 (Le, Ln, Lz)
Chifact	1
Achieved misfit	2034

Table 2. Gravity data, and survey and inversion specifications.

Figure 10 represents a horizontal slice through the gravity inversion at 1100 m. In general, low densities correspond with mapped andesitic volcanic and volcaniclastic units dominating the center of the Buenaventura property. Higher densities in the southwest correlate with mapped plutonic rocks, and to the northeast, correlate with La Negra formation massive andesitic flows. It is possible that the more coherent units are higher density than those which are more fragmental, and likely more porous in nature. A high density ridge extends northeast alongside the interpreted Chivato Fault.

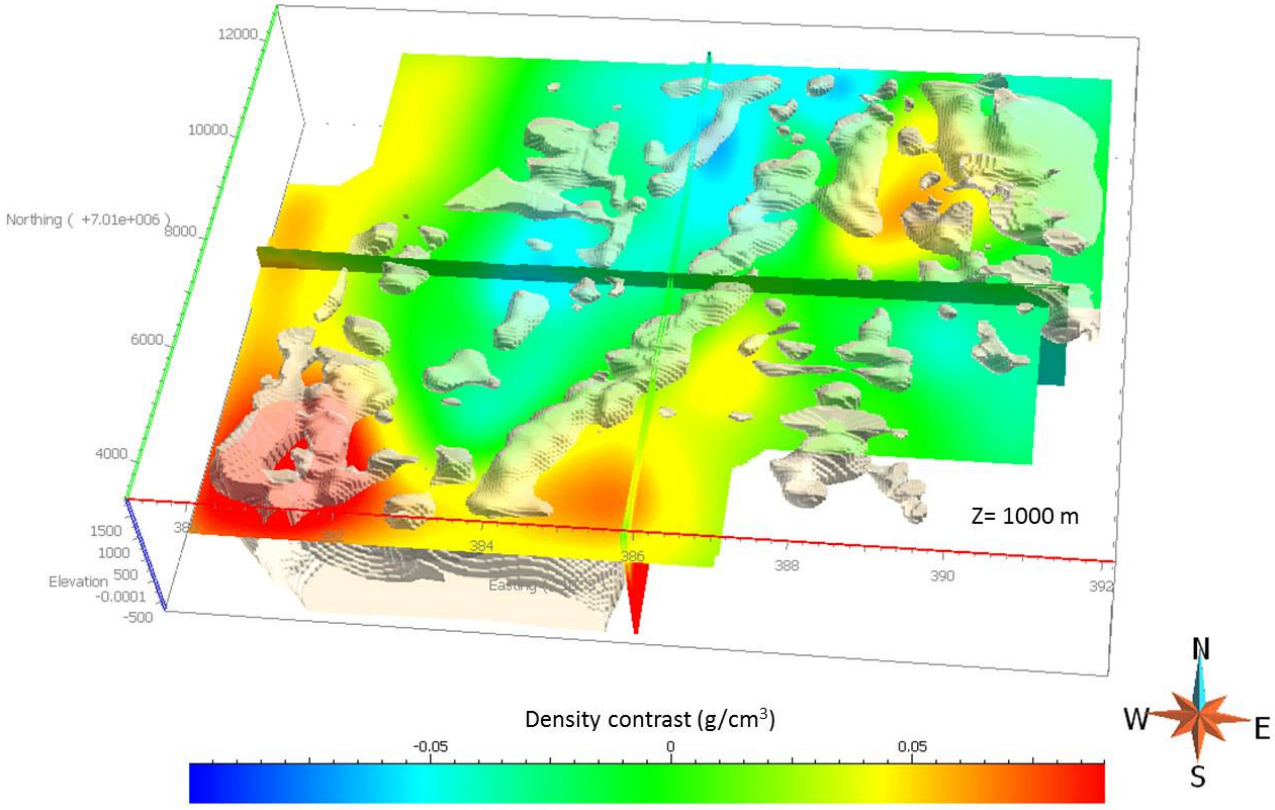

Figure 10. Unconstrained gravity inversion result with magnetic susceptibility isosurface (0.02 S.I. cut-off)

3.2.3 ZTEM Inversion

The Geotech ZTEM data were inverted using UBC-GIF's MT3D code. Figure 11 shows X direction in-phase data at 75 Hz. For pre-processing and inversion parameters see Table 3. For ZTEM inversion modelling, monofrequency inversions were run starting with inversion of 25 Hz data, with each subsequent higher frequency inversion using the previous result as its starting (reference) model. An initial coarsely discretized multifrequency inversion was run using the 600 Hz monofrequency inversion result as its starting model. Finally a finely discretized multifrequency inversion was run using the previous coarsely gridded multi-frequency result as a starting model.

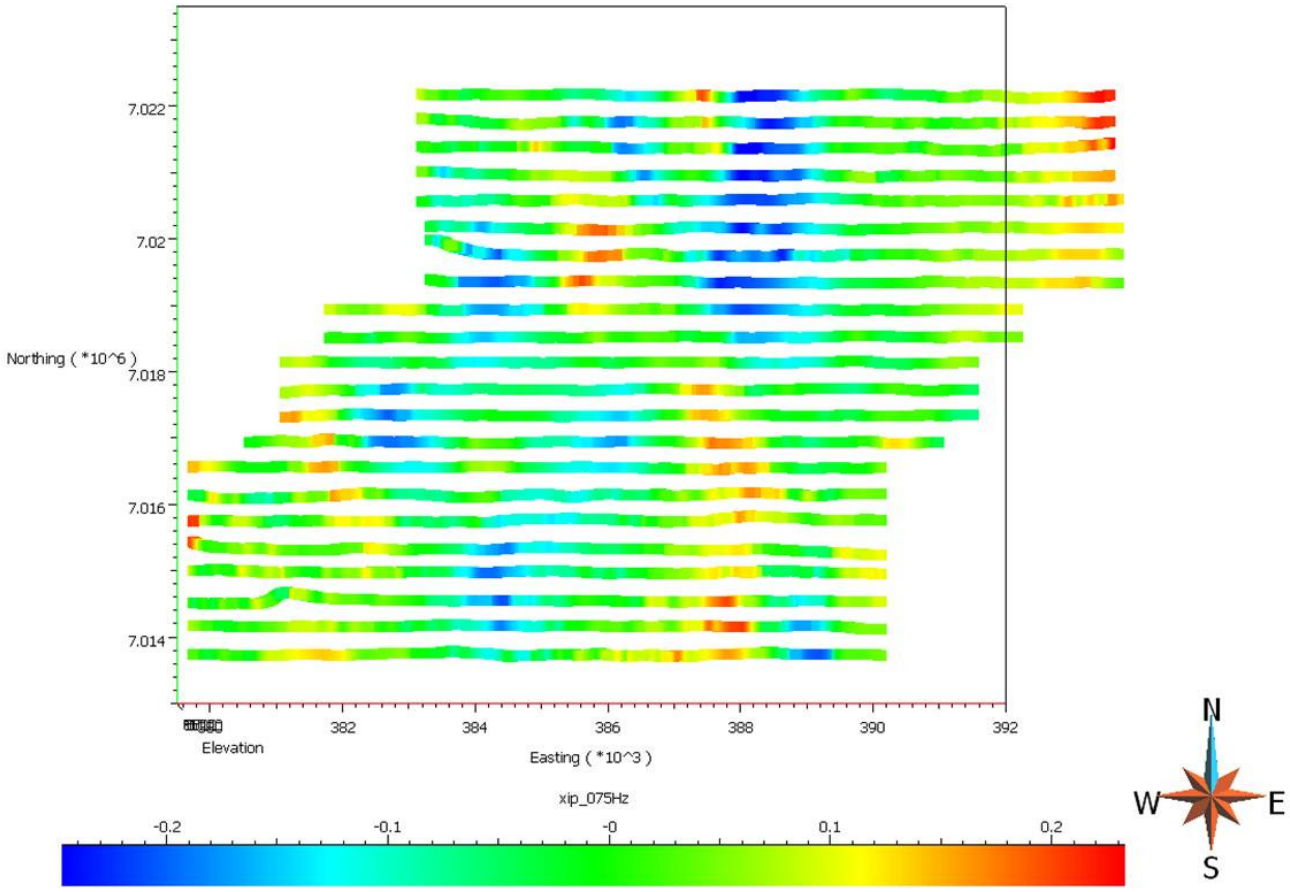

Figure 11. ZTEM X-direction in-phase data at 75 Hz.

Survey specifications	
Survey dates	Jan. 8, 2011 - Jan 18, 2011
Line spacing	400 m
Receiver spacing	9.5 m
Frequencies	25, 37, 75, 150, 300, 600 Hz
Inversion pre-processing	
Coordinate transformation	Rotation from Geotech to EDI system for use in UBC MT3D inversion
Gridded	No
Cultural interference	None obvious
Inversion - combined ground and airborne magnetic data sets	
No. data inverted	591288
Errors	Std dev of 5% of the average value, with a 0.005 floor/minimum value
Mesh core cell sizes	200 x 200 x 50
Length scales	800, 800, 400 (Le, Ln, Lz)
Chifact	1
Achieved misfit	484911

Table 3. ZTEM data, and survey and inversion specifications.

Figure 12 represents a horizontal slice through the ZTEM inversion model at 1100 m. ZTEM inversion results indicate a correlation between high conductivities and areas of thick overburden. Additionally a correlation exists, specifically near surface, with drainage systems mapped on the Quebrada Salitrosa regional map. Conductivity highs otherwise not explained could be related to accumulations of sulfides and/or oxide minerals. Resistive areas generally correlate with outcrop and with intrusive rocks. Robustness of the ZTEM method is verified by visual comparison between geographically registered 2D DC resistivity inversions provided by the client. Consistencies are apparent between shallow EM and DC resistivity results, with both methods effectively discriminating between areas of overburden and outcrop.

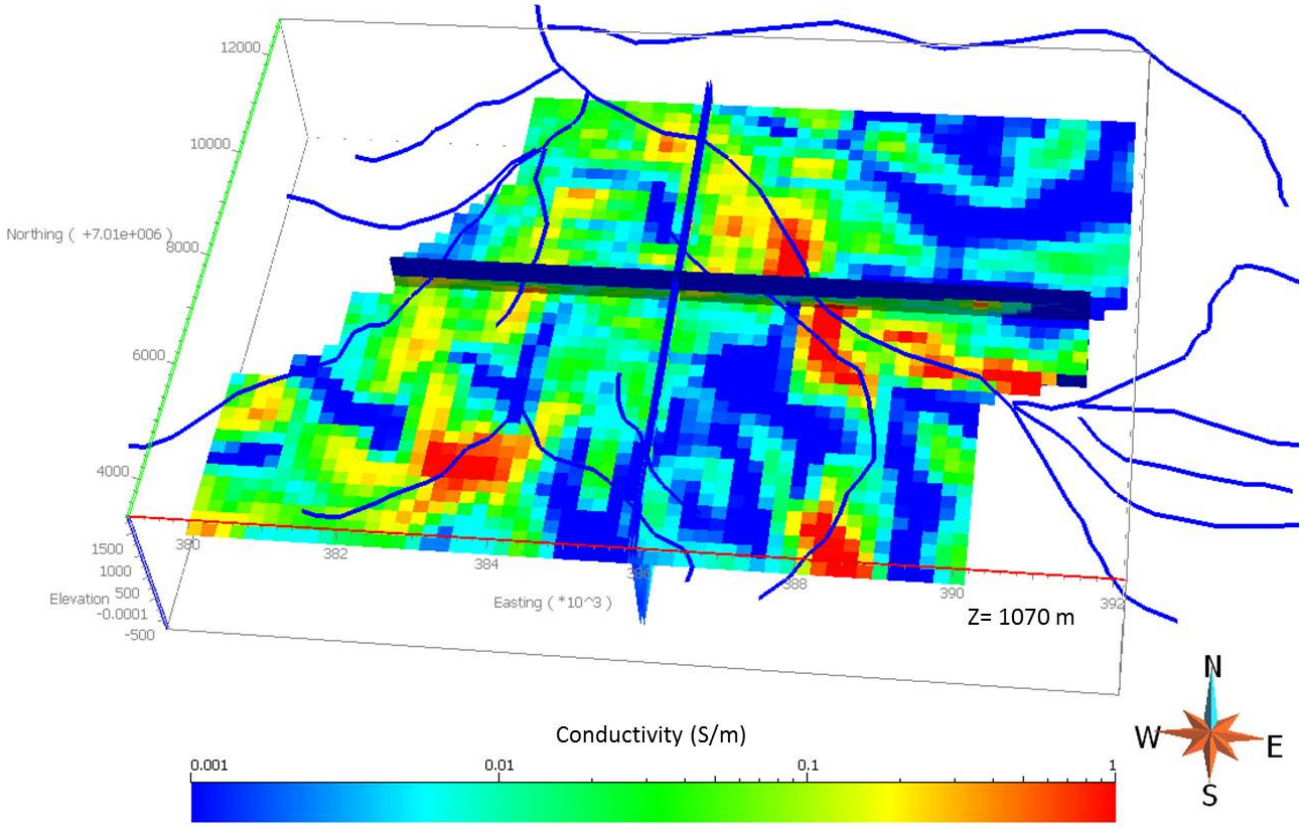

Figure 12. Unconstrained ZTEM inversion result with drainage system overlain.

4 Geological Modelling and Inversion Modelling Stage 2

4.1 3D Geologic Model Construction

Model construction is the process of building a 3D Gocad voxet (block) model of the exploration area and creating the individual exploration criteria as properties of this model. This type of model is termed a Common Earth Model (CEM) because it is meant to be a single model encapsulating all relevant exploration spatial data and spatial interpretation. Geological, geochemical, and geophysical data and interpretation can be queried together. The construction of the final Buenaventura CEM from compiled data and constrained geophysical inversions, and associated challenges are described in the remainder of this section.

4.1.1 Model Design

The 3D geological model was constructed primarily using the preliminary magnetic inversion result guided by downhole physical property data (summarized in Appendix 1), and regional and local geology maps. Structures incorporated include a number of known or interpreted structures recorded on the Buenaventura property map. Small scale faults mapped at the property scale were not included as they were deemed too localized relative to the scale of modelling and targeting. Local faults were not expected to exert significant influence as inversion constraints at the scale of Buenaventura inversions, and if used in targeting as a favorable exploration criteria, would bias results to these well-mapped areas.

The 3D geological and structural model of the Buenaventura property represents a generalized model of geology, and was constructed for the purposes of visual comparison to the various 3D datasets and inversion results, for constraining inversion models, and for targeting. It should be noted that more geological variability (indicated mainly in magnetics, but also shown in drillhole logs) exists than represented in the Gocad model, but with significant overburden and limited drilling, the geology is difficult to confidently interpret. The geological model focuses on five geologic domains, 1) a plutonic domain to the west whose extents were interpreted based on regional and local scale geologic maps, magnetic inversion results, and drillhole logs, 2) a central altered andesitic volcanic/volcaniclastic domain interpreted based on magnetic inversion results, mapping, and drillhole logs, 3) a northeastern unaltered coherent volcanic domain based on mapping and magnetic inversion results, 4) a central buried elongate intrusive interpreted based on magnetic inversion results, and regional scale maps, and 5) overburden interpreted based on gravity inversions, drillhole logs, and mapping.

4.1.2 Modelling process

The general modelling process is outlined below:

- The overburden was modelled as described previously in the depth to bedrock modelling section.
- Mapped contacts (plutonic domain, and 'coherent' volcanic unit) were interpreted through covered areas and were extended to depth guided by the magnetic inversion model result. A magnetic susceptibility isosurface was created at a cut-off of 0.06 SI, and the closed surface thought to represent the extent of the central magnetic zone was extracted and added to the model.
- Constructed surfaces extended downward and outward to the limits of the CEM voxet and were cut against the faces of the voxet and truncated against the top of bedrock surface.
- Faults were created from interpreted fault traces and extended vertically to depth. An exception is the surface representing the eastern edge of Chivato 'deformation zone', where the magnetic inversion suggests a steep easterly dip. The depth cut-offs for the fault planes are based on the source of information.

The 3D geologic model is shown in Figure 13.

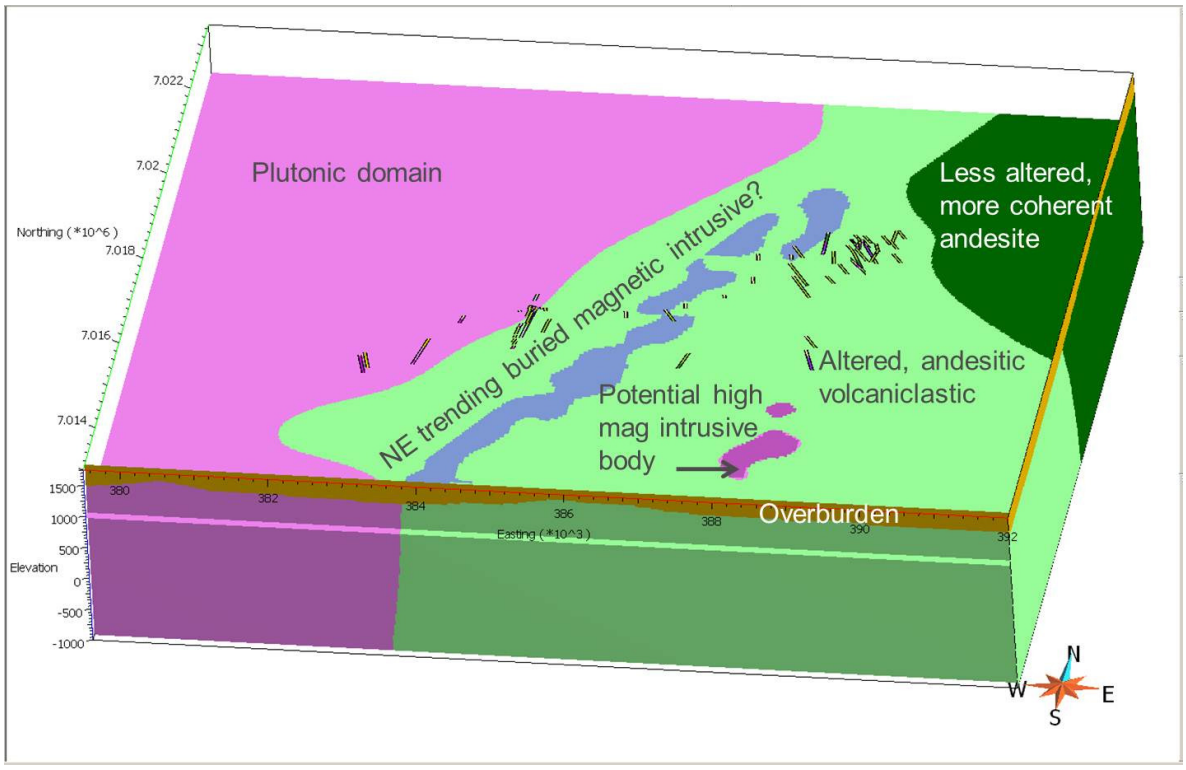

Figure 13. Generalized 3D geology model for the Buenaventura property.

4.1.3 Reference Models

To constrain inversion models, the technique of using a geological model to generate a physical property reference model was applied. Physical property reference models help guide geophysical inversions toward physical property values representing expected geology and structure. The use of bounds models as constraints were also tested. A bounds model specifies the minimum and maximum values allowed within individual cells during inversion calculations. An initial or starting model can be assigned a constant default value, otherwise a previous inversion result or a reference model can act as a starting model. The physical property values assigned to reference and bounds models designed for constraining Buenaventura inversions were based on the assessment of measured downhole physical properties (Appendix A) as well as on general knowledge of rock properties for the known rock types at Buenaventura. Table 4

summarizes physical property values used for constraints, and figures 14-16 show the reference models on the CEM voxet.

Geologic Domains	Mag. Sus. (SI units)		Density contrast (g/cm3)		Conductivity (Ohm-m)	
	reference	*bounds*	*reference (based on avg density of 2.6)*	*bounds*	*reference*	*bounds*
Western plutonic domain	0.05	0-0.5	0.05	-0.2 to +0.6	0.0002	0.0001-0.02
"Altered" volcanic rocks	0.01	0-0.5	0.05	-0.2 to +0.4	0.005	0.0005-2
"Unaltered" volcanic rocks	0.05	0-0.5	0.1	-0.2 to +0.6	0.0002	0.0001-0.02
Central intrusive body	0.1	0-1	0.05	-0.2 to +0.6	0.0002	0.0001-0.02
SE potential small intrusive	0.1	0-1	0.05	-0.2 to +0.6	0.0002	0.0001-0.02
Overburden	0.01	0-0.05	-0.4	-0.6 to -0.2	0.05	0.001-2

Table 4. Physical property values used in reference and bounds models designed to constrain magnetic, gravity and ZTEM inversions

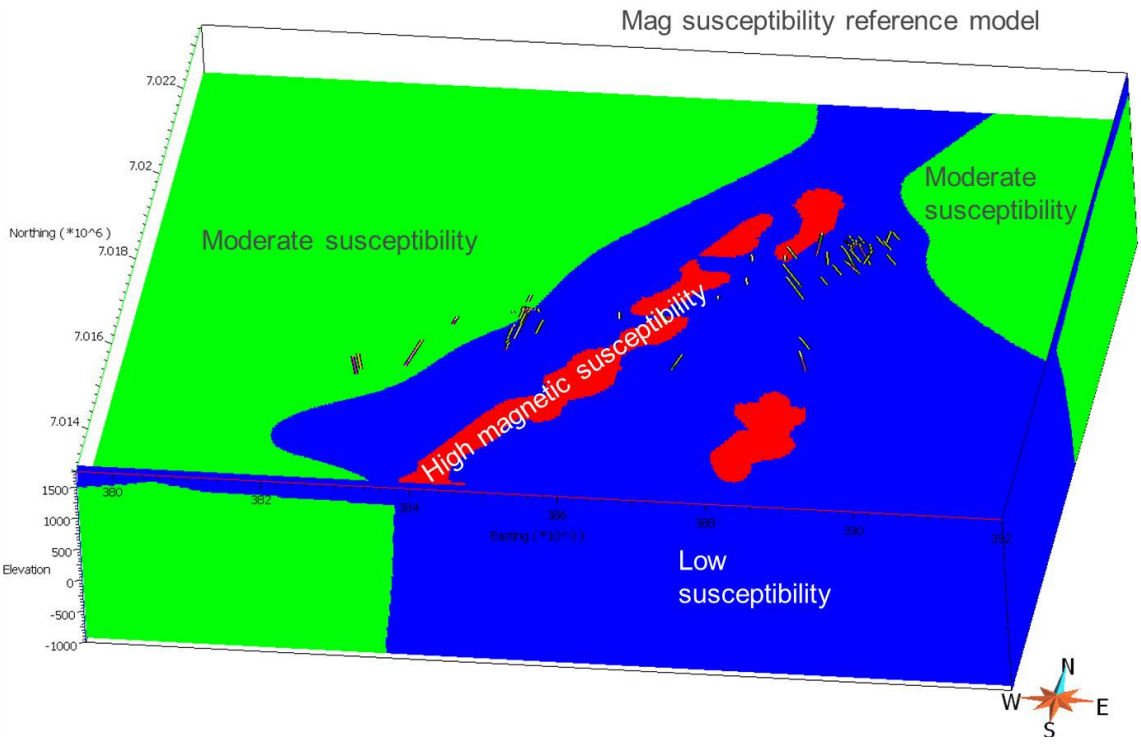

Figure 14. Magnetic susceptibility reference model.

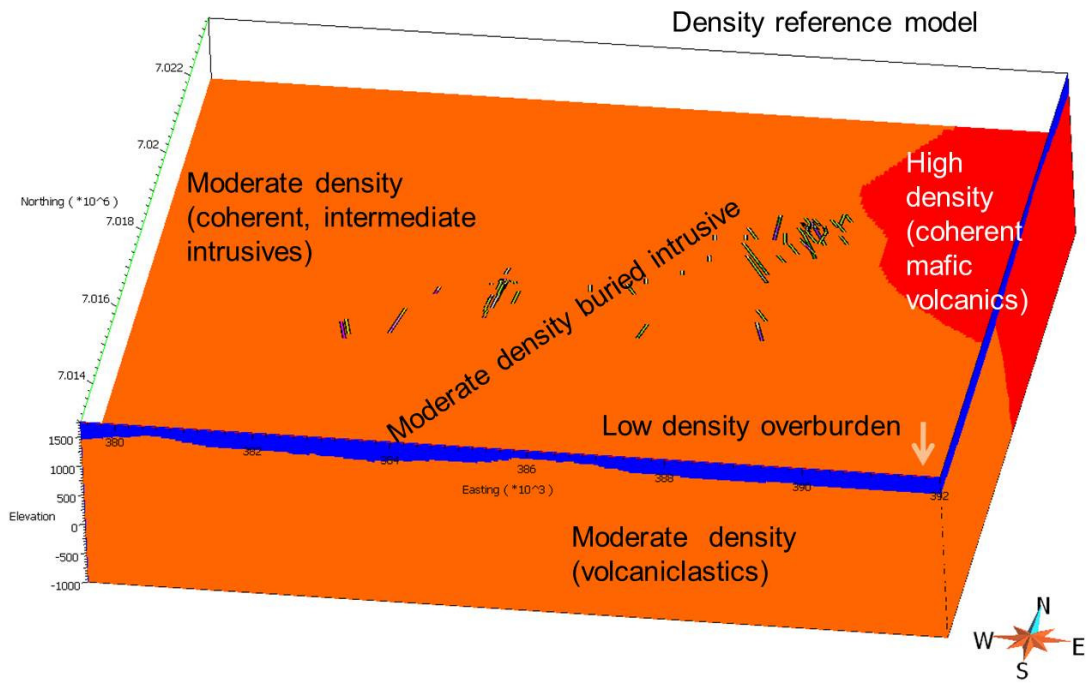

Figure 15. Density contrast reference model.

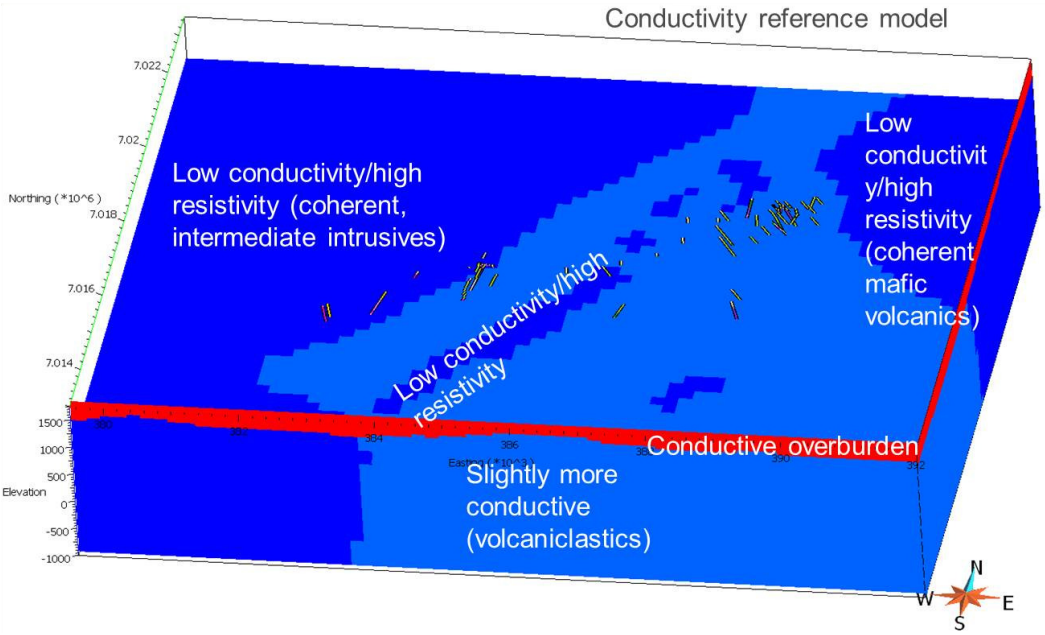

Figure 16. Conductivity reference model.

4.2 Constrained Inversions

4.2.1 Constrained Magnetic Inversion

Various constraints were tested in an attempt to refine the magnetic inversion result. Use of a reference model, use of bounds constraints with a default reference model of 0.001 SI units, and use of combined reference model and bounds constraints was applied. In early constrained magnetic inversions, the initial model was set to a constant default value of 0.001 SI, but this was later replaced by the reference model in an attempt to start the inversion modelling from an expected magnetic susceptibility result. The best constrained magnetic model in this case resulted from use of the geologically derived physical property reference model as both a starting model and a reference model, or 'hypothesis' model, in addition to applying bounds (Figure 17).

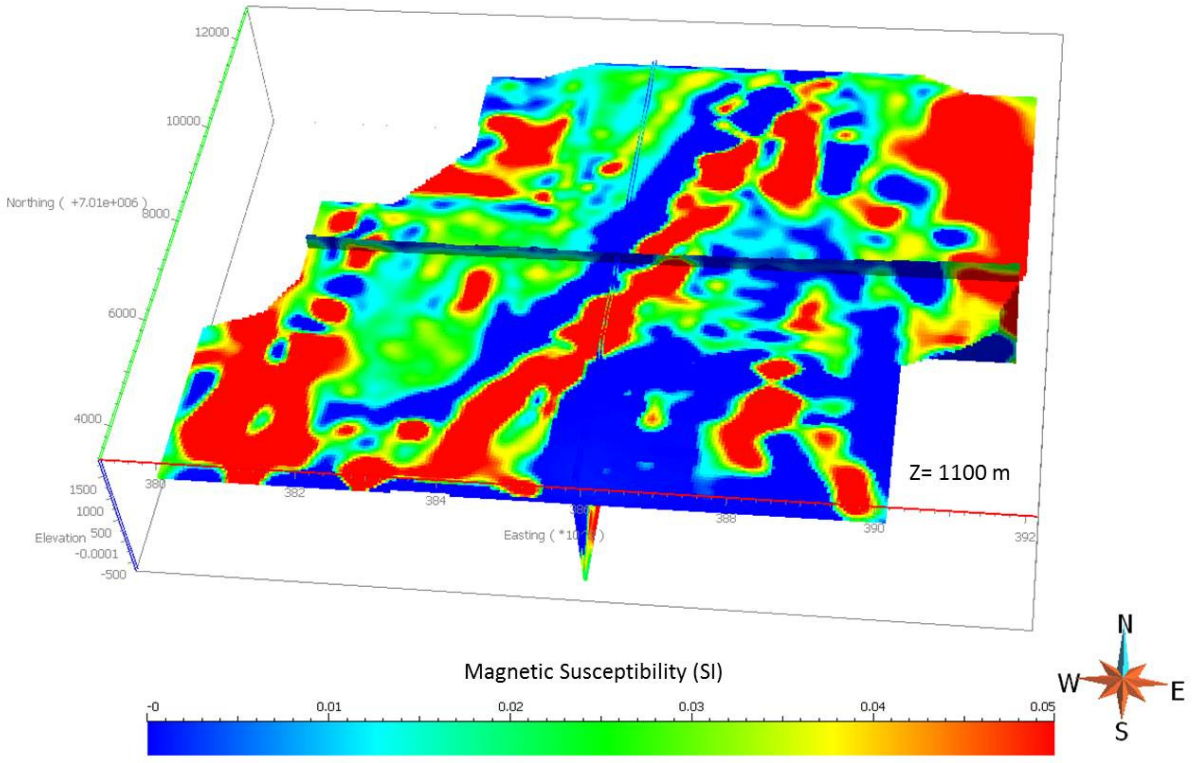

Figure 17. Constrained magnetic inversion result.

The constrained magnetic inversion yields a more smoothly varying model with fewer high frequency and isolated magnetic susceptibility highs. Constraints allowed the magnetic susceptibility within the model to be better distributed to depth, which is thought to be more geologically representative.

4.2.2 Constrained Gravity Inversion

As for magnetic inversions, various constraining parameters were tested to refine the gravity inversion result. The best result came from use of bounds along with a reference model set at the default value 0 g/cm^3 for gravity inversions (Figure 18). The application of these constraining parameters served to bring out more detail in the density contrast model, especially near surface, while still fitting the observed gravity data. The largest influence on the refinement of the result is likely the acknowledgement by the bounds model of the low density overburden expected near surface.

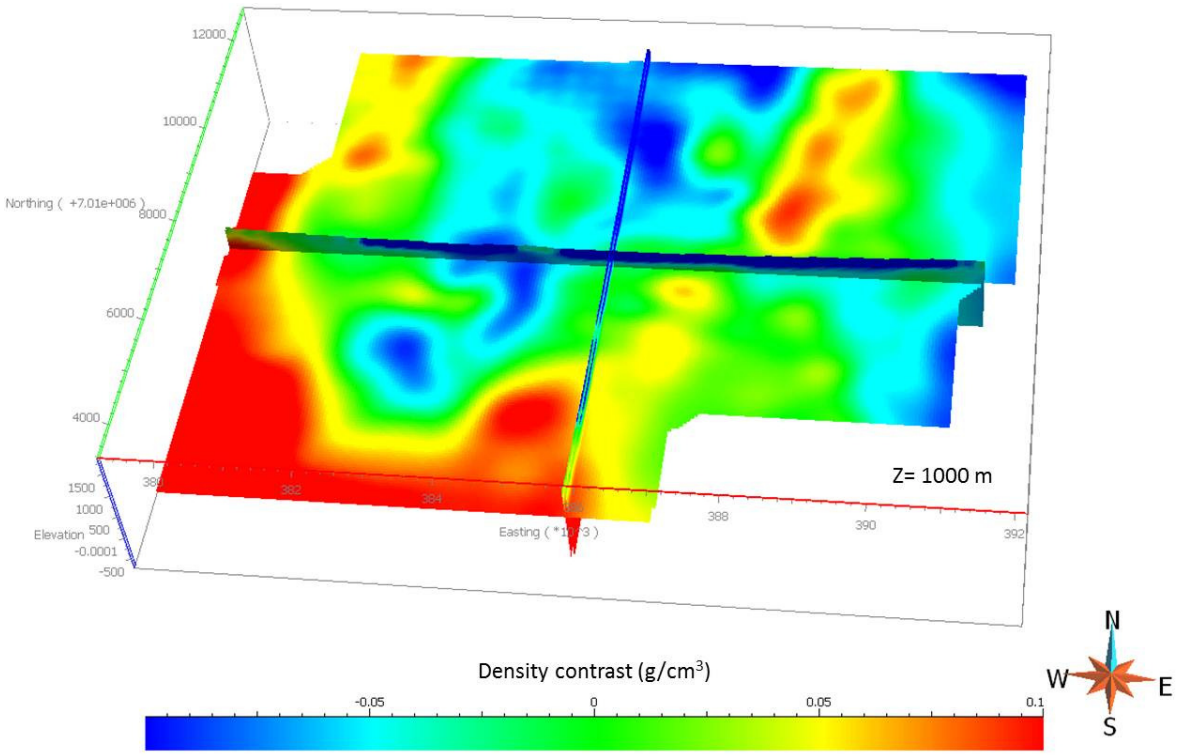

Figure 18. Constrained gravity inversion.

4.2.3 Attempts to Constrain ZTEM Inversions

Although an attempt was made to constrain the ZTEM inversion using the geologically derived conductivity reference model, the result was unsatisfactory. The reason for this is that the 3D geologic model does not appropriately represent the conductivity distribution at Buenaventura. As discussed in an earlier section of this report covering initial inversion results, conductivity modelled at Buenaventura seems to be generally related to more recent geology, following drainage systems, faults, and reflecting overburden layers. Low conductivity (high resistivity) material may correspond well generally with coherent intrusive rock, however the interference of cross-cutting conductive features limits the use of a lithologic model alone as a constraint. A more thorough understanding of the causes of high conductivities at Buenaventura may be helpful in development of more useful ZTEM constraints.

5 Targeting

5.1 Exploration Criteria for Targeting at Buenaventura

At the onset of the project, Mira Geoscience was invited by Cliffs Natural Resources to attend an IOCG deposit workshop presented by mineral exploration consultant Murray Hitzman. After this course, Mira Geoscience collaborated with the clients to build a set of applicable generalized, and more property-specific, IOCG exploration criteria which would serve as a basis for the knowledge-driven targeting to be eventually applied to the Buenaventura CEM.

The following is a list of exploration criteria compiled at the onset of the Buenaventura targeting project. Underlying notes indicate the capacity in which the criteria were applied to guide the targeting. Some of these criteria were changed or modified as the project progressed and if this was the case, the reasons are described.

1. *Rock type.* The favoured deposit emplacement lithologies are (Punta del Cobre) andesitic volcanics, and then intrusives. A 3D geological model was constructed based on existing mapping, drillholes logs, and initial interpretation of unconstrained geophysical inversions. So as not to rule out any lithologies as potential hosts, instead of targeting specific lithologies

interpreted within the targeting volume, geology was targeted indirectly using geophysics. In this setting, the rock properties constitute a more important criteria than interpreted geology with the combination of high magnetic susceptibility, density, and conductivity being the highest priority target, presumably reflecting alteration and mineralization characterized by the presence of abundant Fe-oxides and sulphide minerals. Though the 3D geologic model is not directly targeted, proximity to hydrothermal and tectonic breccia bodies will however constitute a lithological criteria as described in 3.

2. *Proximal to major deep structures (NW, NS, NE in order of importance).* Structures were modelled in 3D based on a combination of data, such as direct field mapping, remote sensing image interpretation, magnetic map interpretation, and magnetic inversion interpretation. The Chilean IOCG belt shows fundamental control by high-angle, crustal-scale structures (many linked to the Atacama Fault Zone). Northwest trending faults will be grouped and given higher weightings, while north and northeast trending faults will be assigned slightly lower weightings for targeting. Fault intersections are also considered important for localization of metal-bearing fluids.

3. *Proximity to brecciated rocks*. Hydrothermal-magmatic breccias are common hosts to IOCG mineralization. Breccia intervals have been logged in several drillholes on the property and proximity to these intervals will be favoured in targeting. It was initially proposed that known brecciation zones would be modelled in 3D. Although hydrothermal and tectonic breccias have been logged from drillcore, and were mapped in the Cerro Breccia area, the distribution is variable and localized, and difficult to trace. In addition these occurrences represent very small features relative to the scale of the model volume. It was thought that breccia bodies might appear as lower density and higher conductivity features in inversions, allowing subsurface modelling, but again scale is a limitation, as well, altered rock (and other geological features such as faults) might have similar characteristics.

4. *Within regional sodic alteration, proximal to or directly associated with potassic (or possibly calcic or hydrolytic) alteration.* Regional sodic alteration defines the “fairways” for exploration, while potassic alteration is expected to be restricted to the immediate vicinity of

the deposit, typically having an area in plan of less than 10 km^2. Hydrolytic or HSCC (hematite-sericite-carbonate-chlorite) alteration, although not ubiquitously associated with IOCG deposits, may occur very proximal to the ore, at a high elevation in the system. Because of the generally pervasive hydrolytic alteration of the Punta del Cobre volcanic rocks dominating the central Buenaventura property, with no obvious centers of more intense potassic alteration, mapped alteration was not deemed to be a useful targeting parameter to include within the model. Additionally, targeting using mapped alteration would bias the results toward outcropping rocks. Alteration will, to some degree, be represented within inversion results, where magnetic highs can signify secondary magnetite alteration. Although surface alteration was not used explicitly in targeting, downhole alteration, represented as visual mineral estimates downhole, is used as a targeting criteria, as is discussed in 5 below.

5. *Proximal to pyrite.* Presence and intensity of pyrite, and other metallic minerals, were logged downhole during past drilling programs. Key alteration minerals reflective of IOCG deposit magmatic-hydrothermal systems were additionally logged. IOCG style mineralization might be indicated by the occurrence of sulphides (chalcopyrite, pyrite), and Fe-oxides (magnetite, hematite). Alteration minerals typically characterizing hydrothermal centers include sericite, K-feldspar, biotite, and chlorite. The final targeting strategy will involve a criteria weighted in favour of proximity to the presence of each of these minerals of interest.

6. *Geochemical vectors.* Geochemical data of various types have been collected on the Buenaventura property (e.g. MMI survey, drillhole, trenching). Based on correlations of elements and mineralization at known IOGC deposits, as well as on potentially interesting relationships apparent from visual inspection and trends within downhole and MMI geochemistry, a suite of elements was chosen for targeting. A selection of elements measured during MMI surveying will be targeted included Ag, As, Au, Ba, Cd, Cs, Cu, Mn, P, and Zn. Downhole ICP-MS data also provides a large suite of elements for use in targeting. The downhole elements of interest for this targeting exercise include Au, As, Fe, Co, and Cu.

7. *Direct deposit detection through anomalous geophysical response or physical property signature.* A significant IOCG deposit is expected to have an anomalous geophysical

response because it will represent a large volume of material (characterized by secondary magnetite, hematite, and sulfides) with anomalously high density, magnetic susceptibility, and electrical conductivity with respect to the host rock environment. Constrained 3D inversions of gravity, magnetic, and ZTEM help to best infer a deposit directly.

5.2 Knowledge-based Targeting in 3D: the Targeting Workflow

Knowledge-driven targeting algorithms (along with weights-of-evidence algorithms) have been built into a Gocad workflow plug-in: the Targeting Workflow. The workflow is implemented as a series of sequential panels (Figure 19) where the user is required to select data objects and other required input before proceeding to the next step. Software workflows in general are beneficial in that they allow practitioners to execute complex 3D quantitative processes yielding robust, consistent and repeatable results. This ensures the domain-expert thought process is captured and followed by the workflow user which in turn ensures rigorous application of the statistical methods.

Figure 20 depicts, as an example, the input data and results of a knowledge-based targeting model computed using the Targeting Workflow for the Buenaventura property. The user is guided through reclassifying continuous and discrete variables into several classes or binary properties (Figure 20 a-f) and through execution of the targeting algorithm to produce the mineral potential model (Figure 20 g).

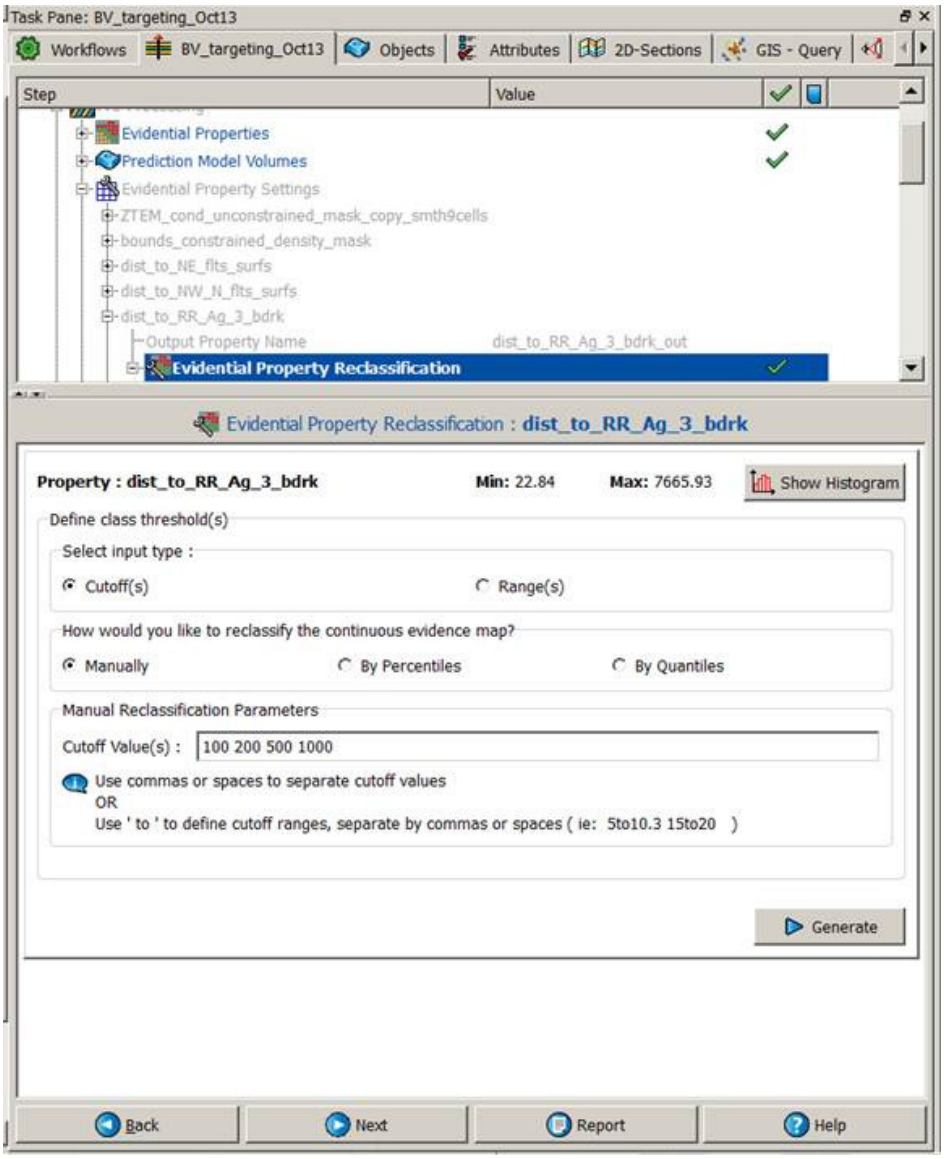

Figure 19. One of the decision panels from the Gocad Targeting Workflow. Note the list of completed tasks at the top and user input in the bottom section.

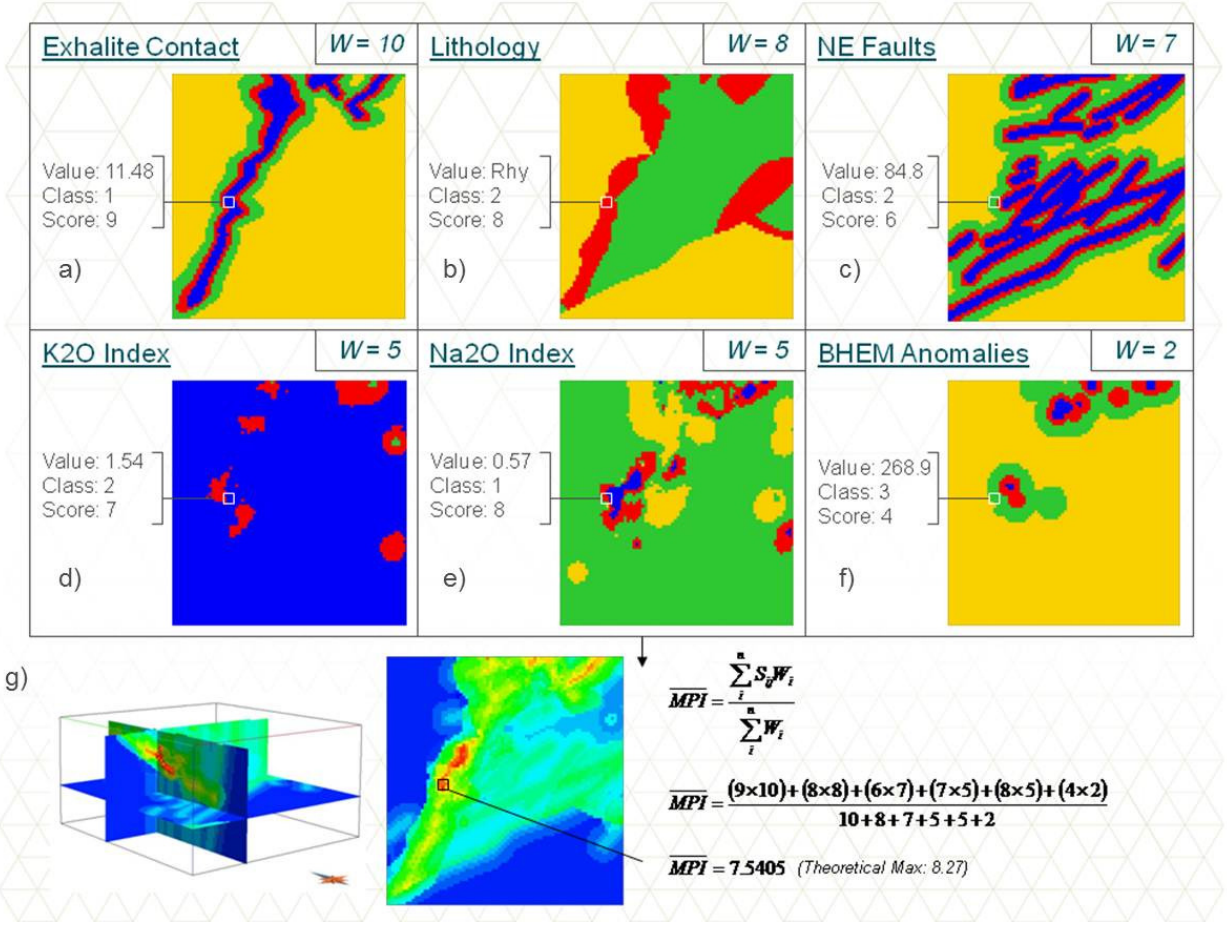

Figure 20. Example of targeting for the Ribago district in the central Noranda camp, Quebec; showing input evidential properties (a-f) and the resultant mineral potential model (g).

5.3 Targeting at Buenaventura

The Gocad Targeting Workflow was applied to systematically identify targets within the Buenaventura property from multiple relevant geological, geochemical, and geophysical datasets projected onto the Common Earth Model.

Datasets relevant to the exploration criteria are compiled and represented on a targeting voxet quantitatively. Table 5 summarizes the criteria used in targeting at Buenaventura and describes how each criteria are represented on the targeting voxet.

Exploration criteria	Representation on targeting voxet
Geological Criteria	
Proximity to magmatic-hydrothermal breccia	Distance to downhole mbh intervals
Proximity to tectonic breccia	Distance to downhole mbt intervals
Structural Criteria	
Proximity to NE trending faults/structures	Distance to NE trending fault surfaces
Proximity to NW and N trending faults/structures	Distance to NW and N trending fault surfaces
Proximity to fault intersections	Distance to fault intersections (3D)
Mineralogical Criteria	
Alteration indicator - presence of biotite	Distance to downhole biotite (present)
Mineralization - presence of chalcopyrite	Distance to downhole cpy (present)
Alteration indicator - presence of Fe-oxides	Distance to downhole hematite and or magnetite
Alteration indicator - presence of K-feldspar	Distance to downhole K-feldspar
Mineralization - presence of pyrite	Distance to downhole pyrite
Geochemical Criteria	
Anomalous metals from MMI - Ag	Distance to MMI Ag RR >/= 3 ppb (projected to bedrock)
Anomalous metals from MMI - As	Distance to MMI As RR >/= 1.5 ppb (projected to bedrock)
Anomalous metals from MMI - Au	Distance to MMI Au RR >/= 8 ppb (projected to bedrock)
Alteration indicator from MMI - Ba	Distance to MMI Ba RR >/= 3 ppb (projected to bedrock)
Anomalous metals from MMI - Cd	Distance to MMI Cd RR >/= 2 ppb (projected to bedrock)
Anomalous metals from MMI - Co	Distance to MMI Co RR >/= 5.5 ppb (projected to bedrock)
Anomalous metals from MMI - Cu	Distance to MMI Cu RR >/= 2.9 ppb (projected to bedrock)
Alteration indicator from MMI - K	Distance to MMI K RR >/= 2.3ppm (projected to bedrock)
Alteration indicator from MMI - Mn	Distance to MMI Mn RR >/= 4.5 ppb (projected to bedrock)
Alteration indicator from MMI - P	Distance to MMI P RR >/= 6 ppm (projected to bedrock)
Anomalous metals from MMI - Zn	Distance to MMI Zn RR >/= 2.6 ppb (projected to bedrock)
Anomalous metals from ICP-MS - As	Distance to downhole As >/= 15 ppm
Anomalous metals from ICP-MS - Au	Distance to downhole Au >/= 0.037 ppm
Anomalous metals from ICP-MS - Co	Distance to downhole Co >/= 119 ppm
Anomalous metals from ICP-MS - Cu	Distance to downhole Cu >/= 0.1 %
Anomalous metals from ICP-MS - Fe	Distance to downhole Fe >/= 11 %
Geophysical Criteria	
High magnetic susceptibility	Magnetic susceptibility model from magnetic inversion, constrained withinitial model, reference model, and bounds
High conductivity	Conductivity model from ZTEM inversion, smoothed to reduced noise in model at surface
High density	Density contrast model from gravity inversion, constrained with bounds and default reference model

Table 5. Exploration criteria used in targeting at Buenaventura. Geochemical thresholds are set using either the 80th or 90th percentile.

Continuous and discrete evidential properties are converted to several classes or to binary properties for the current implementation of the Targeting Workflow. Distance properties generated on the targeting voxet which measure distance to favourable faults, anomalous geochemistry, alteration, and sulphide and oxide mineralogy are subdivided into classes based on the anticipated influence of that criteria on surrounding rocks. For example, if being close to a fault constitutes prospectivity, a cell between 0 and 50 m of a fault might be considered very prospective, a cell between 50 m and 200 m, somewhat prospective, while cells greater than 200 m away may be deemed to have a low prospectivity. In this example, there would be three classes set for the distance-to-fault property. Figure 21 shows the property 'Distance to anomalous Ag', as well as the reclassification of this property into four classes, with the proximal red zones to eventually be scored higher than those zones with increasing distance to the anomalous cell.

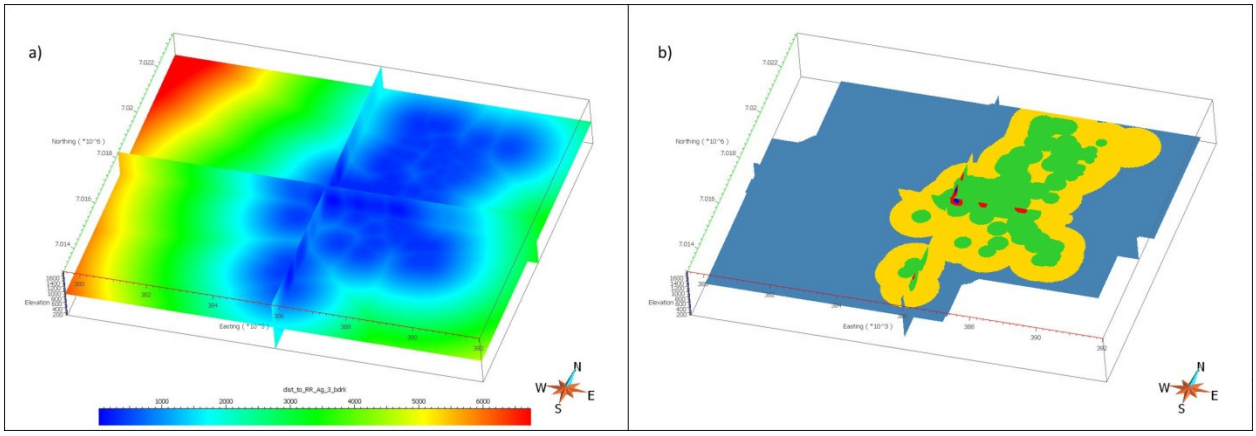

Figure 21. Example of a) the property 'distance to anomalous Ag' and b) classes assigned based on increasing distance from the prospective feature.

Geophysical inversions are reclassified as binary properties on the targeting voxet where the inversion model is divided into two classes based upon a threshold or cut-off value that best separates regions of the grid containing anomalous values from those regions containing non-anomalous values (Figure 22). Weights are then assigned to the various exploration criteria,

followed by assignment of scores to the subdivided classes. Physical property and geochemical cut-offs representing anomalous values, distance thresholds, and weights and scores were decided on through discussions with the client.

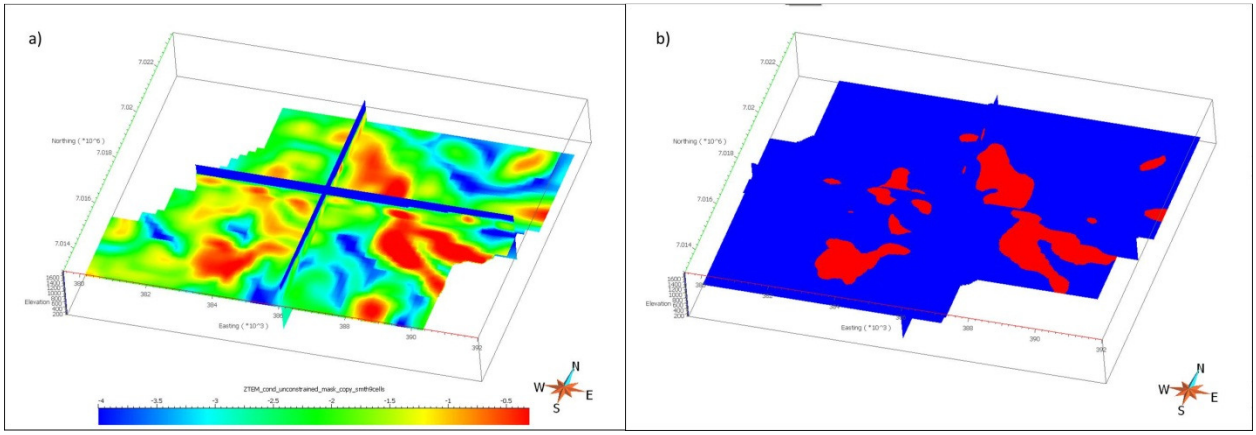

Figure 22. Example of a geophysical inversion property (conductivity) reclassified as a binary property.

The targeting method chosen is a knowledge-based method. Exploration criteria and related weights are assigned based on expert input. A weights-of-evidence approach was not a valid option for this project due to a lack of training areas – known mineralization on the Buenaventura property may not accurately reflect the range of mineralization styles on the property. By using the knowledge-based approach, a more generalized view can be taken and a wider range of targets can be identified if the expert so chooses, with criteria selected appropriately.

Three models, exploring results from different combinations of criteria, are presented to the client. The following sections outline the targeting results.

5.3.1 Model 1 – All Criteria Used

For the first targeting session, all criteria contained on the targeting voxet were used. This means that there will inevitably be some bias toward existing drilling sites, as well as MMI sampling

sites. However, only those holes having anomalous geochemistry or containing favorable metals or alteration minerals will contribute to a positive result, potentially giving some indication where future infill drilling can be directed. Table 6 summarizes Model 1 criteria and weights, and Figures 23 and 24 depict Model 1 results.

Targeting Criteria - Model 1	Weight	Classes	Scores
Geological Criteria			
Distance to downhole mbh intervals	4	0-100 m, 100-200m, 200-500m, >500m	4,3,1,0,0
Distance to downhole mbt intervals	4	0-100 m, 100-200m, 200-500m, >500m	4,3,1,0,0
Structural Criteria			
Distance to NW and N trending fault surfaces	5	0-100m, 100-200m, 200-500m, 500-1000m, >1000m	4,3,2,1,0
Distance to fault intersections (3D)	5	0-100m, 100-200m, 200-500m, 500-1000m, >1000m	4,3,2,1,0
Distance to NE trending fault surfaces	4	0-100m, 100-200m, 200-500m, 500-1000m, >1000m	4,3,2,1,0
Mineralogical Criteria			
Distance to downhole cpy (present)	4	0-100 m, 100-200m, 200-500m, >500m	4, 3, 1, 0, 0
Distance to downhole hematite and or magnetite	3	0-100 m, 100-200m, 200-500m, >500m	4, 3, 1, 0, 0
Distance to downhole biotite (present)	3	0-100 m, 100-200m, 200-500m, >500m	4, 3, 1, 0, 0
Distance to downhole K-feldspar	3	0-100 m, 100-200m, 200-500m, >500m	4, 3, 1, 0, 0
Distance to downhole pyrite	2	0-100 m, 100-200m, 200-500m, >500m	4, 3, 1, 0, 0
Geochemical Criteria			
Distance to downhole Au >/= 0.037 ppm	3	0-100 m, 100-200m, 200-500m, >500m	4, 3, 1, 0, 0
Distance to downhole Cu >/= 0.1 %	3	0-100 m, 100-200m, 200-500m, >500m	4, 3, 1, 0, 0
Distance to downhole Fe >/= 11 %	3	0-100 m, 100-200m, 200-500m, >500m	4, 3, 1, 0, 0
Distance to downhole Co >/= 119 ppm	2	0-100 m, 100-200m, 200-500m, >500m	4, 3, 1, 0, 0
Distance to downhole As >/= 15 ppm	2	0-100 m, 100-200m, 200-500m, >500m	4, 3, 1, 0, 0
Distance to MMI Ag RR >/= 3 ppb (projected to bedrock)	2	0-100 m, 100-200m, 200-500m, >500m	4, 3, 1, 0, 0
Distance to MMI As RR >/= 1.5 ppb (projected to bedrock)	2	0-100 m, 100-200m, 200-500m, >500m	4, 3, 1, 0, 0
Distance to MMI Au RR >/= 8 ppb (projected to bedrock)	2	0-100 m, 100-200m, 200-500m, >500m	4, 3, 1, 0, 0
Distance to MMI Co RR >/= 5.5 ppb (projected to bedrock)	2	0-100 m, 100-200m, 200-500m, >500m	4, 3, 1, 0, 0
Distance to MMI Cu RR >/= 2.9 ppb (projected to bedrock)	2	0-100 m, 100-200m, 200-500m, >500m	4, 3, 1, 0, 0
Distance to MMI Ba RR >/= 3 ppb (projected to bedrock)	1	0-100 m, 100-200m, 200-500m, >500m	4, 3, 1, 0, 0
Distance to MMI Cd RR >/= 2 ppb (projected to bedrock)	1	0-100 m, 100-200m, 200-500m, >500m	3, 2, 1, 0, 0
Distance to MMI K RR >/= 2.3ppm (projected to bedrock)	1	0-100 m, 100-200m, 200-500m, >500m	4, 3, 1, 0, 0
Distance to MMI Mn RR >/= 4.5 ppb (projected to bedrock)	1	0-100 m, 100-200m, 200-500m, >500m	3, 2, 1, 0, 0
Distance to MMI P RR >/= 6 ppm (projected to bedrock)	1	0-100 m, 100-200m, 200-500m, >500m	3, 2, 1, 0, 0
Distance to MMI Zn RR >/= 2.6 ppb (projected to bedrock)	1	0-100 m, 100-200m, 200-500m, >500m	4, 3, 1, 0, 0

Targeting Criteria - Model 1 (continued)	Weight	Classes	Scores
Geophysical Criteria			
Magnetic susceptibility model from magnetic inversion, constrained with initial model, reference model, and bounds	5	<0.06, >0.06 SI	0, 4
Conductivity model from ZTEM inversion, smoothed to reduced noise in model at surface	5	<0.02, >0.02 S/m	0, 4
Density contrast model from gravity inversion, constrained with bounds and default reference model	5	<0.1, >0.1 g/cm^3	0, 4

Table 6. Exploration criteria, weights, classes, and scores applied for generation of targeting Model 1.

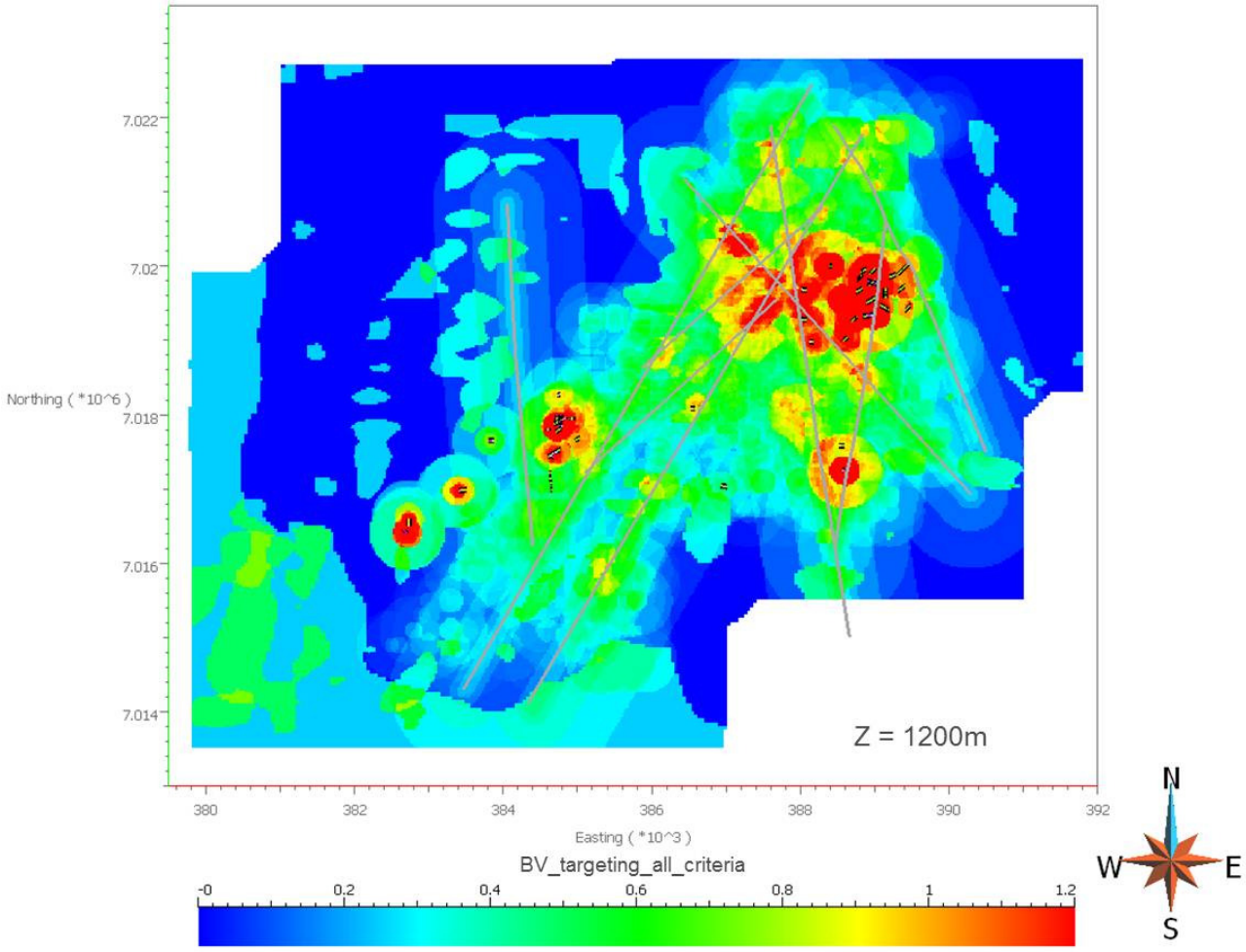

Figure 23. Model 1, horizontal slice through the mineral potential index volume. Drillholes and select fault traces shown.

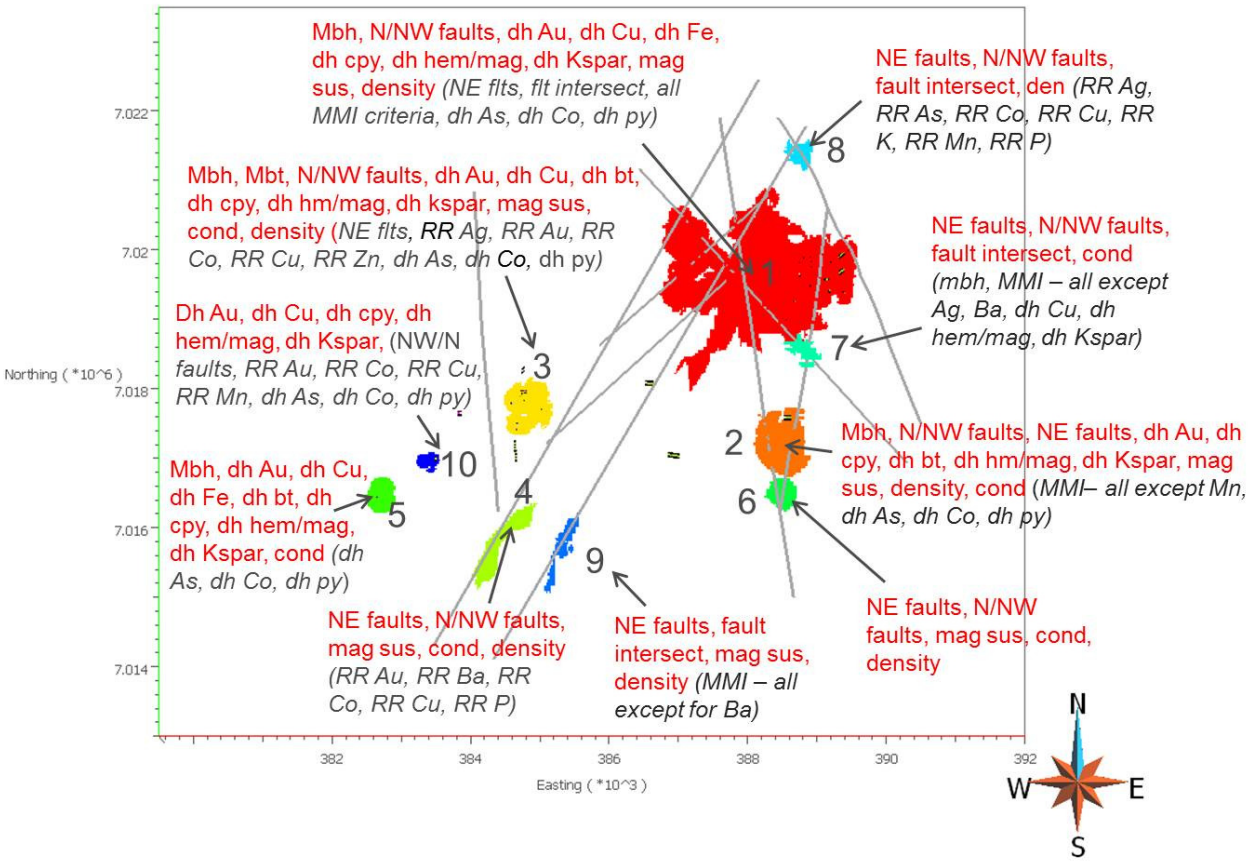

Figure 24. Model 1, top ten target regions with most influential contributing criteria in red type, and less influential criteria in black (For details on contributing criteria, see Appendix 2). Drillholes and select fault traces shown.

5.3.2 Model 2 – Drillhole Data Removed from Targeting

All downhole data was eliminated during the second targeting session to remove drilling bias. MMI data are retained in an attempt to highlight possible areas of interest away from outcrop in areas of cover. Table 7 summarizes Model 2 criteria and weights, and Figures 25 and 26 depict Model 2 results.

Targeting Criteria - Model 2	Weight	Classes	Scores
Structural Criteria			
Distance to NW and N trending fault surfaces	5	0-100m, 100-200m, 200-500m, 500-1000m, >1000m	4,3,2,1,0
Distance to fault intersections (3D)	5	0-100m, 100-200m, 200-500m, 500-1000m, >1000m	4,3,2,1,0
Distance to NE trending fault surfaces	4	0-100m, 100-200m, 200-500m, 500-1000m, >1000m	4,3,2,1,0
Geochemical Criteria			
Distance to MMI Ag RR >/= 3 ppb (projected to bedrock)	2	0-100 m, 100-200m, 200-500m, >500m	4, 3, 1, 0, 0
Distance to MMI As RR >/= 1.5 ppb (projected to bedrock)	2	0-100 m, 100-200m, 200-500m, >500m	4, 3, 1, 0, 0
Distance to MMI Au RR >/= 8 ppb (projected to bedrock)	2	0-100 m, 100-200m, 200-500m, >500m	4, 3, 1, 0, 0
Distance to MMI Co RR >/= 5.5 ppb (projected to bedrock)	2	0-100 m, 100-200m, 200-500m, >500m	4, 3, 1, 0, 0
Distance to MMI Cu RR >/= 2.9 ppb (projected to bedrock)	2	0-100 m, 100-200m, 200-500m, >500m	4, 3, 1, 0, 0
Distance to MMI Ba RR >/= 3 ppb (projected to bedrock)	1	0-100 m, 100-200m, 200-500m, >500m	4, 3, 1, 0, 0
Distance to MMI Cd RR >/= 2 ppb (projected to bedrock)	1	0-100 m, 100-200m, 200-500m, >500m	3, 2, 1, 0, 0
Distance to MMI K RR >/= 2.3ppm (projected to bedrock)	1	0-100 m, 100-200m, 200-500m, >500m	4, 3, 1, 0, 0
Distance to MMI Mn RR >/= 4.5 ppb (projected to bedrock)	1	0-100 m, 100-200m, 200-500m, >500m	3, 2, 1, 0, 0
Distance to MMI P RR >/= 6 ppm (projected to bedrock)	1	0-100 m, 100-200m, 200-500m, >500m	3, 2, 1, 0, 0
Distance to MMI Zn RR >/= 2.6 ppb (projected to bedrock)	1	0-100 m, 100-200m, 200-500m, >500m	4, 3, 1, 0, 0
Geophysical Criteria			
Magnetic susceptibility model from magnetic inversion, constrained withinitial model, reference model, and bounds	5	<0.06, >0.06 SI	0, 4
Conductivity model from ZTEM inversion, smoothed to reduced noise in model at surface	5	<0.02, >0.02 S/m	0, 4
Density contrast model from gravity inversion, constrained with bounds and default reference model	5	<0.1, >0.1 g/cm^3	0, 4

Table 7. Exploration criteria, weights, classes, and scores applied for generation of targeting Model 2.

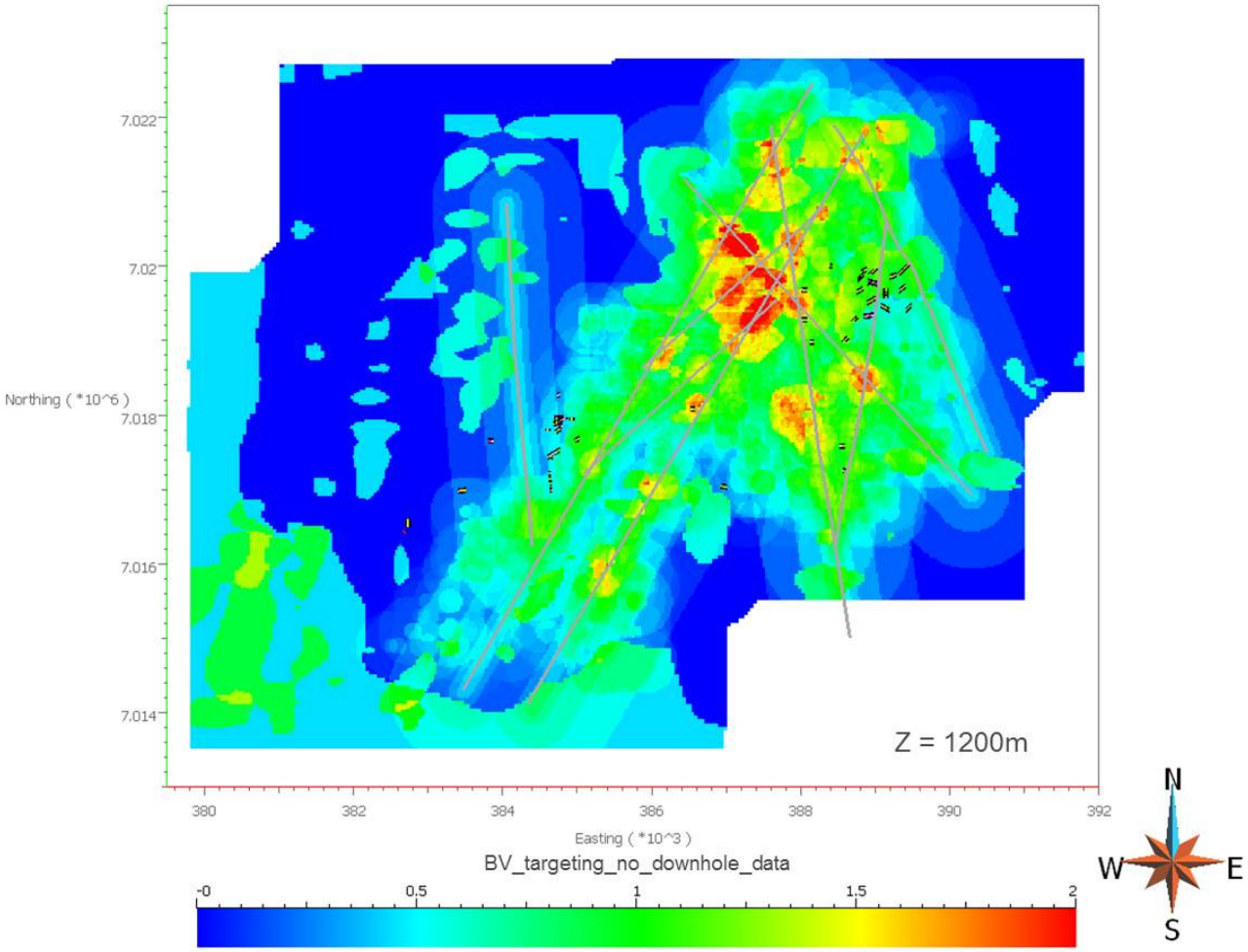

Figure 25. Model 2, horizontal slice through the mineral potential index volume. Drillholes and select fault traces shown.

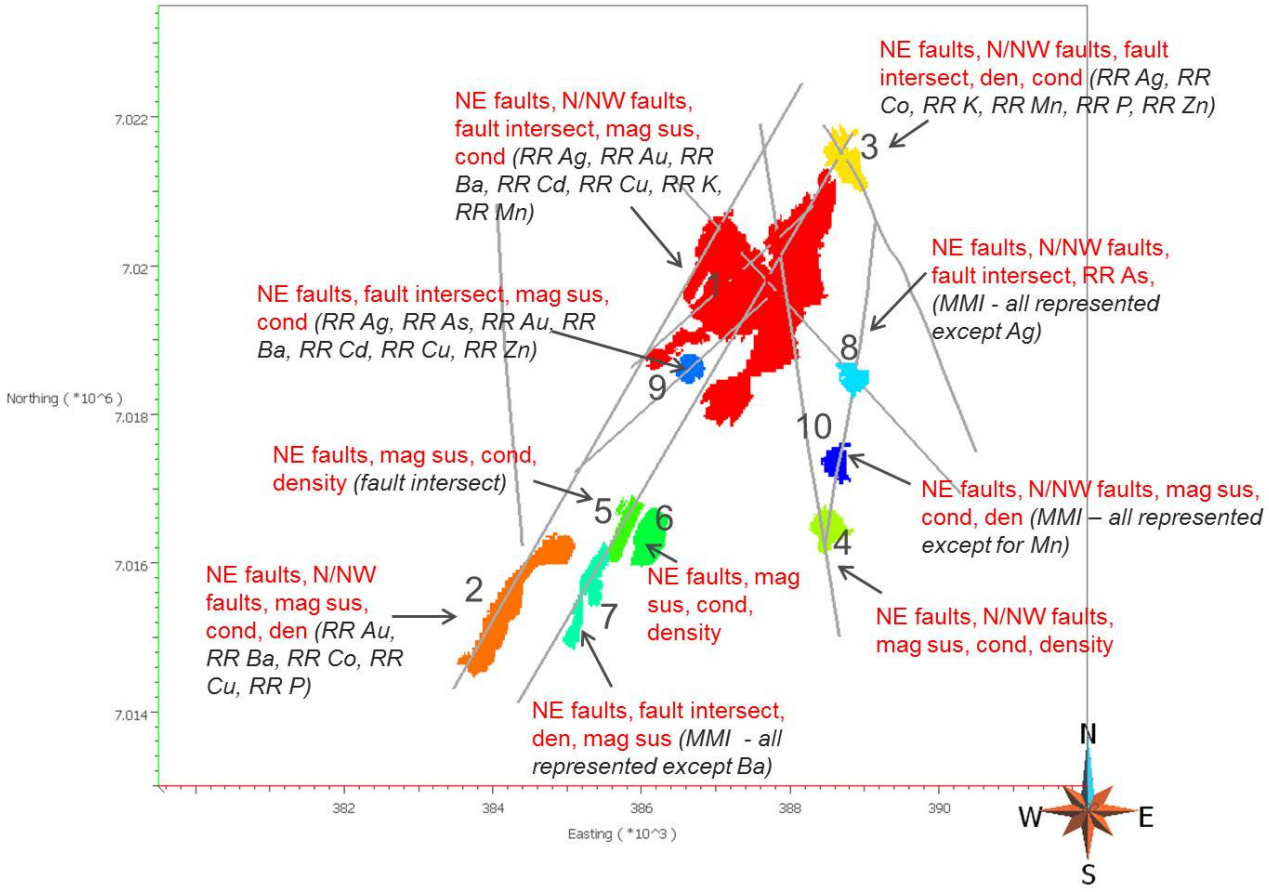

Figure 26. Model 2, top ten target regions with most influential contributing criteria in red type, and less influential criteria in black (For details on contributing criteria, see Appendix 2). Drillholes and select fault traces shown.

5.3.3 Model 3 – Geophysical Inversions and Faults (no downhole data, no MMI data)

The third targeting session removes downhole geochemical and mineral data and MMI geochemistry, leaving only geophysical inversion results and interpreted faults as exploration criteria. Table 8 summarizes Model 3 criteria and weights, and Figures 27 and 28 depict Model 3 results.

Targeting Criteria - Model 3	Weight	Classes	Scores
Structural Criteria			
Distance to NW and N trending fault surfaces	5	0-100m, 100-200m, 200-500m, 500-1000m, >1000m	4,3,2,1,0
Distance to fault intersections (3D)	5	0-100m, 100-200m, 200-500m, 500-1000m, >1000m	4,3,2,1,0
Distance to NE trending fault surfaces	4	0-100m, 100-200m, 200-500m, 500-1000m, >1000m	4,3,2,1,0
Geophysical Criteria			
Magnetic susceptibility model from magnetic inversion, constrained withinitial model, reference model, and bounds	5	<0.06, >0.06 SI	0, 4
Conductivity model from ZTEM inversion, smoothed to reduced noise in model at surface	5	<0.02, >0.02 S/m	0, 4
Density contrast model from gravity inversion, constrained with bounds and default reference model	5	<0.1, >0.1 g/cm^3	0, 4

Table 8. Exploration criteria, weights, classes, and scores applied for generation of targeting Model 2.

6 Conclusions

- Mira Geoscience has successfully compiled numerous disparate datasets from the Buenaventura property into a consistent 3D Common Earth Model. Three physical property models were generated through geophysical inversion of magnetic, gravity, and ZTEM data and are incorporated into the CEM. The 3D CEM provides a highly effective medium for visualizing, querying, and interpretation of multiple data sets at once.
- Inversion models provide a more direct spatial link to geology than raw geophysical data. The three inversion models generated can be used independently to improve understanding of geology under Quaternary cover rocks on the Buenaventura property, and to refine an evolving 3D geologic model. Magnetic susceptibility may be useful for mapping out least-altered volcanic rocks, magnetite-bearing intermediate to mafic intrusive rocks, and zones of secondary magnetite related to alteration. Conductivity models indicate drainage systems, structure, and potentially outline more resistive coherent intrusive rocks. Density appears to distinguish between coherent least-altered

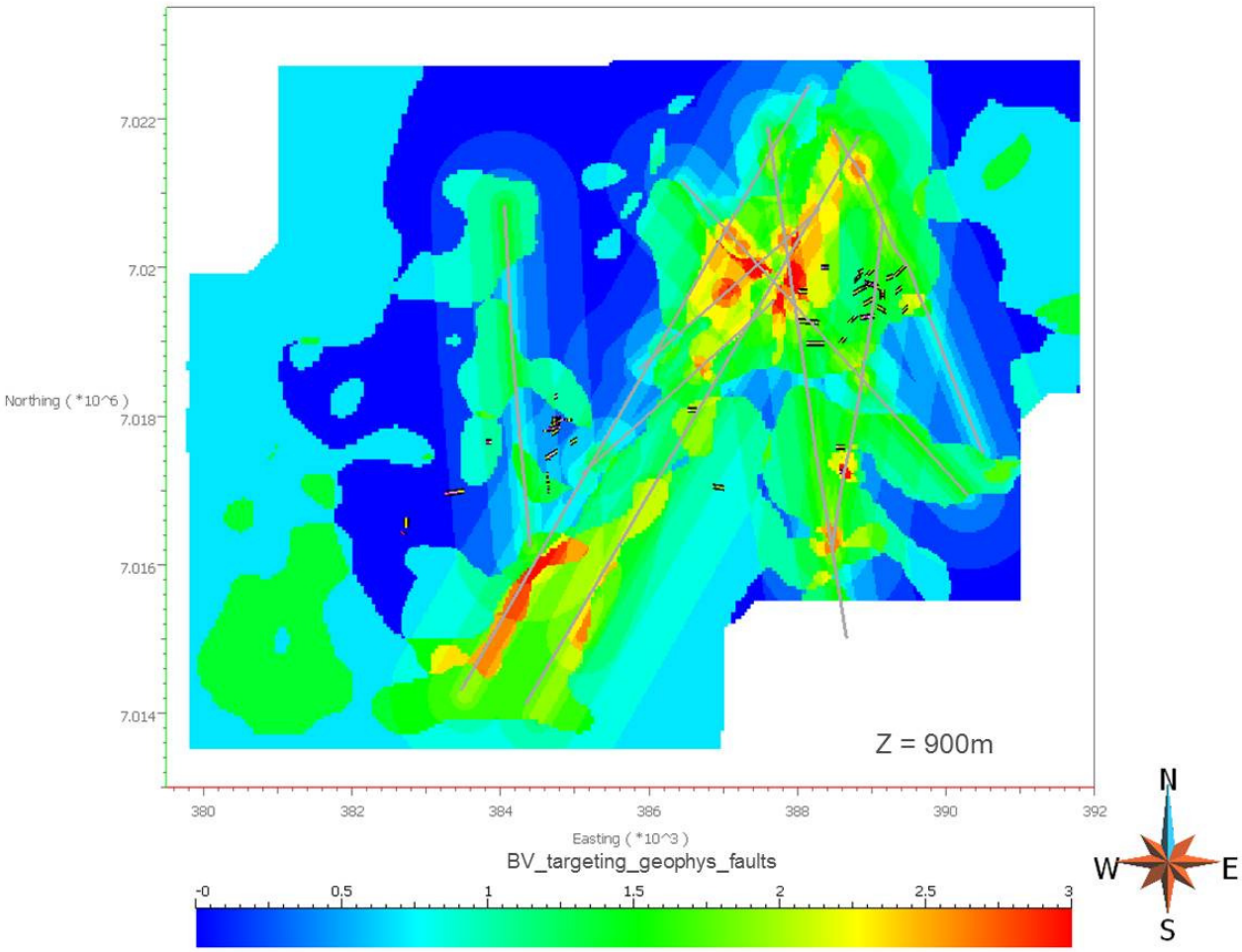

Figure 27. Model 3, horizontal slice through the mineral potential index volume. Drillholes and select fault traces shown.

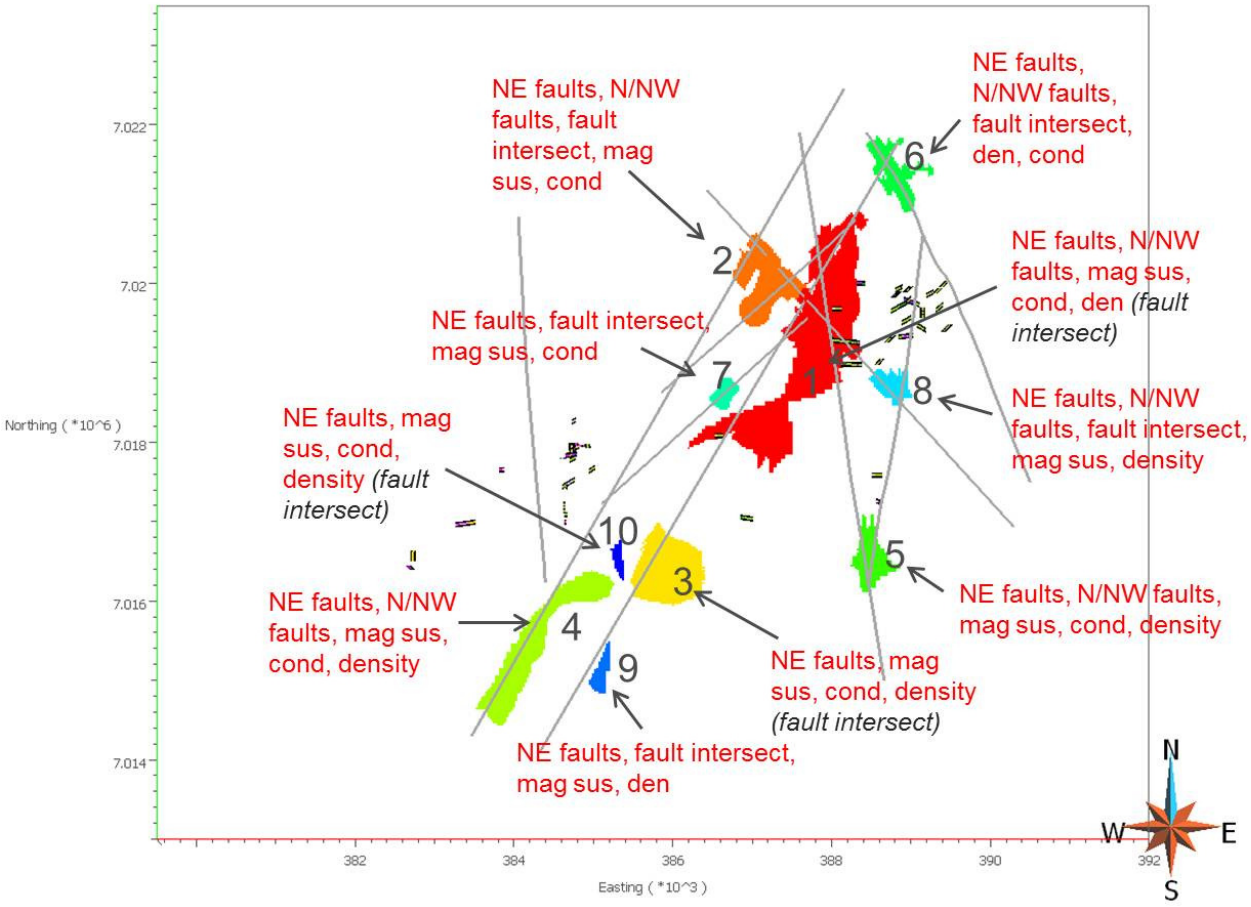

Figure 28. Model 3, top ten target regions with most influential contributing criteria in red type, and less influential criteria in black (For details on contributing criteria, see Appendix 2). Drillholes and select fault traces shown.

rocks, and more porous, altered, or brecciated lithologies. Although each inversion result contributes clues to buried geology, inversion models are most powerful when interpreted together. Querying several 3D physical property models along with geological and geochemical data within a Common Earth Model provides an effective means of interpreting geological and alteration patterns, and assessing mineral exploration potential.

- The Gocad Targeting Workflow employed by Mira Geoscience for this project provides an objective method of 3D exploration targeting, offering the best chance to find mineralization based on a given set of exploration criteria. The Targeting Workflow is

not a 'black box' method. It applies established and easily understood methods of rating the mineral potential of cells making up the targeting volume. Mineral potential index values are output, as are the various criteria scores. As such, it is possible to explore the result in terms of the degree to which each criteria has contributed to a target, so that each target may be fully understood.

- Three targeting results are delivered, each based on a different combination of exploration criteria. Model 1 includes drillhole data, biasing targeting toward previous drilling, but highlighting those drilled areas which are most prospective (characterized by the greatest number of overlapping favourable criteria). Model 2 removes drillhole influence, but keeps MMI geochemical criteria, highlighting prospective areas masked by cover rocks. Model 3 uses only geophysical criteria and interpreted faults. This model specifically highlights structures coinciding with zones of high magnetic susceptibility, high density, and high conductivity, which are thought to reflect expected physical property characteristics of IOCG style mineralization.
- Those areas consistently highlighted through the different targeting results include the area to the north and northwest of previous drilling at Cerro Brecha, where numerous structures intersect, and high density, susceptibility, and conductivity material is modelled. With downhole data considered, the cells surrounding holes BV10DD02, BH-01, 02 and 03 are highlighted. Another area consistently highlighted corresponds to favourable structural and geophysical features east of Loma Negra near holes BH-04 and BV10DD01. Model cells situated approximately 1000 m south of these holes, near the property boundary, are also highlighted. Numerous zones are targeted along the central high magnetic susceptibility body where high densities and conductivities overlap with high susceptibility material and with inferred structures. One of the stronger anomalies of this type occurs along the western margin of the magnetic body in the southwestern part of the property.
- Tierra Noble's current drilling program will provide ground-truthing of geophysical models and interpreted geology. Specific geophysical or geochemical methods useful in identifying mineralization or fingerprinting lithologic units might be chosen again to be

applied for mapping and exploration in geologically analogous terranes. If targeting based on the methods described herein proves to be successful in identifying new mineralization on the Buenaventura property, it might suggest future application of a similar workflow using similar parameters in comparable geological settings within which IOCG deposits are expected to occur.

- Finally, the Common Earth Model produced in this study should have persistent value to Tierra Noble as long as they hold the property. Modifications to exploration criteria or target type, definition of training data, or simply the addition of new drilling or other data can all be used to update the existing model easily now that the investment in the 3D model framework for Buenaventura is complete.

7 Deliverables

The project deliverables include

- Geophysical inversion results in UBC-GIF format (mesh and model files). UBC-GIF Meshtools3D can be downloaded free from: http://www.eos.ubc.ca/ubcgif/ (under Software – Utility Codes). Meshtools3D can be used to view slices of the models, change data scales, and generate isosurfaces to explore physical property distributions in 3D.
- Targeting Workflow report (html file) indicating targeting criteria used, and weights and scores assigned
- Target profile sheets with spatial information and contributing criteria associated with the top 10 target centroids for each model
- XYZ file containing spatial data and scores related to the top 10 target centroids
- DXF shell files representing the top 10 targeting regions
- 3D pdfs showing the top 10 target regions from each model

8 Recommendations

The following outlines recommendations for future work on the Buenaventura property based on the modelling and targeting results presented herein.

Physical properties

A better physical property dataset would aid greatly in interpreting geophysical inversion models, and in deciding on thresholds and cut-off values for targeting. Additionally, physical property data can be used in constraining future inversion models. Due to limited drilling coverage, and limited downhole physical property data, physical property characteristics for the full range of rock types and alteration assemblages are not understood. To enhance physical property knowledge it is suggested that magnetic susceptibility and density measurements be taken on old drillholes. It might be beneficial to send a smaller representative suite of samples to a laboratory for collection of electrical properties to determine relative differences between mineralized and barren, and coherent and brecciated rock types. Additional rock property information for intrusive rocks is important since multiple intrusive phases are mapped near the western and southern edges of the Buenaventura property, some of which appear to be more magnetic than others. Physical property measurements on outcrop or outcrop samples would be useful in adding to the physical property knowledge base, but also could be used to constrain near-surface cells during inversion, which can significantly improve the estimation of physical properties in cells at depth in the inversion.

Borehole geophysics would be an effective means to collect detailed physical property data. Having numerous rock property variables means that if one property does not detect variation between two rocks or two styles of alteration, there may be another which can more effectively do so. This information can be valuable for planning future geophysical surveys.

Lithogeochemistry

Physical rock properties information can help with interpretation of geophysical inversion to unravel geology in areas covered by overburden. Lithogeochemical data can also be interrogated to understand geology and alteration in covered areas. Geochemical analyses from hand samples from regular sampling of outcrops may be helpful in enhancing knowledge of geochemical patterns related to mineralization and alteration. To most effectively interpret geochemical patterns and to appropriately define anomalies, it is essential to first have a solid understanding of background geochemical signals. Geochemical analyses on a sample suite collected from unaltered Punta del Cobre volcanic rocks could shed light on the degree of alteration on the Buenaventura property. Physical property data can also be analyzed alongside geochemical data to determine if there are trends that could allow for one parameter to act as proxy for another.

Mapping

With a significant portion of the property covered by alluvial and fluvial sediments, the geology is difficult to fully resolve. It is likely that most outcrops on the property have been mapped. Due to a lack of understanding of the cause of strong density and susceptibility anomalies found in the southwest, it is recommended that an attempt be made to investigate the intrusive rocks which are mapped in this area on regional maps, and an effort be made to compare these rocks to intrusive rocks on the property. Although officially south of the property, investigating geology here could help with interpretations of inversion models within property bounds.

Geophysics

Areas consistently highlighted through the various targeting sessions could warrant more localized geophysical data collection in order to refine the dimensions and extents of apparent mineralization. If drilling successfully intersects mineralization there, smaller scale surveys might be considered for targeted areas northwest of Cerro Breccia, east of Loma Negra, or over

highlighted zones along the northeast trending magnetic zone, where mineralization may be focused by contacts or structures.

Targeting

If a consistent style of mineralization is uncovered on the Buenaventura property, and if there is developed a more accurate idea of the distribution of barren versus mineralized rock, the client may wish to apply weights of evidence methods in targeting, whereby established mineralized zones can act as training areas from which exploration criteria are derived.

3D Model

For best interpretation and review capability, it is recommended that Tierra Noble purchase a Gocad viewer. The project can then be packaged and delivered to the client in its entirety and inversion model results, geologic models, drillhole and surface data, and target regions can be viewed together.

9 References

Apel M., and Böhme, M., 2006, Predictive 3D mineral potential modelling. Proc. 26th Gocad Research Consortium Meeting, Nancy, France.

Bonham-Carter, G.F., 1994, Geographic Information Systems for Geoscientists: Modelling with GIS: Pergamon Press.

Bonham-Carter, G.F., 1997, GIS methods for integrating exploration data sets, in Gubins, A.G., ed., Proceedings of Exploration 97: Fourth Decennial Conference on Mineral Exploration, 59-64.

Caumon, G., Ortiz, J., and Rabeau, O., 2006, A comparative study of three mineral potential mapping techniques, Proc. IAMG 2006.

Marschik, R. and Fontboté, L., 2001, The Candelaria-Punta del Cobre iron oxide Cu-Au(-Zn-Ag) deposits, Chile. Economic Geology, 96, no 8, pp1799-1826.

Appendix 1. Downhole magnetic susceptibility and density data

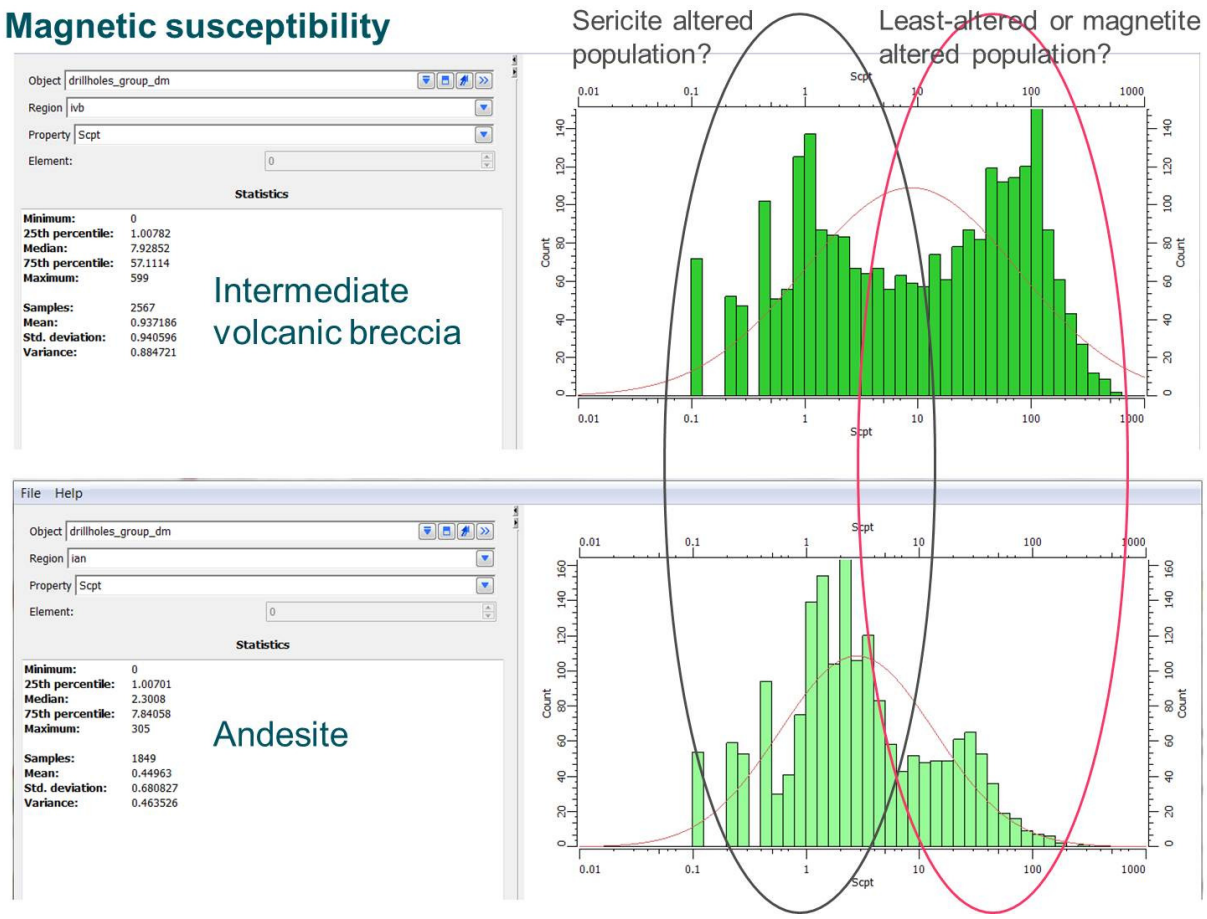

Figure 29. Summary statistics and histograms summarizing magnetic susceptibility data collected from intermediate volcanic rock samples.

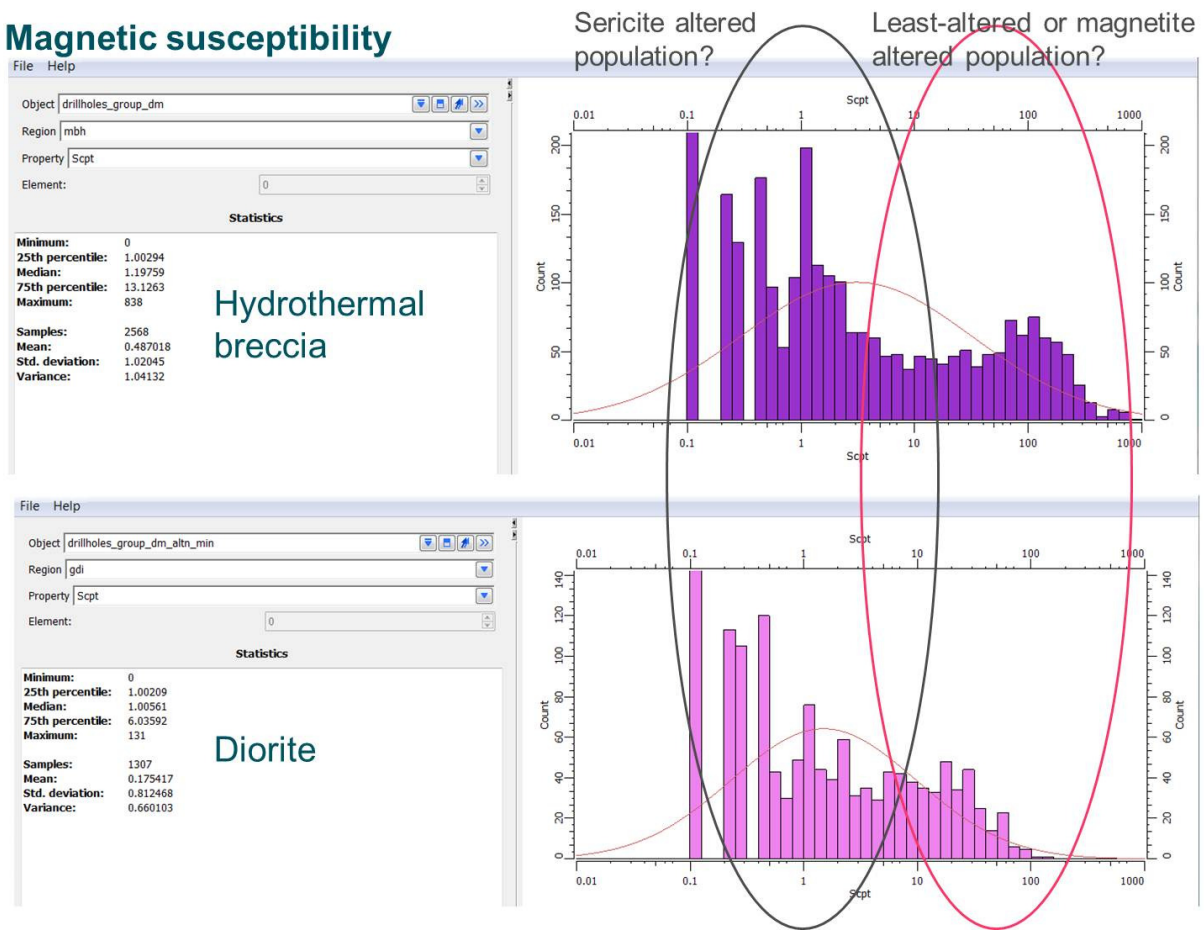

Figure 30. Summary statistics and histograms summarizing magnetic susceptibility data collected from hydrothermal breccia and diorite intrusive rocks.

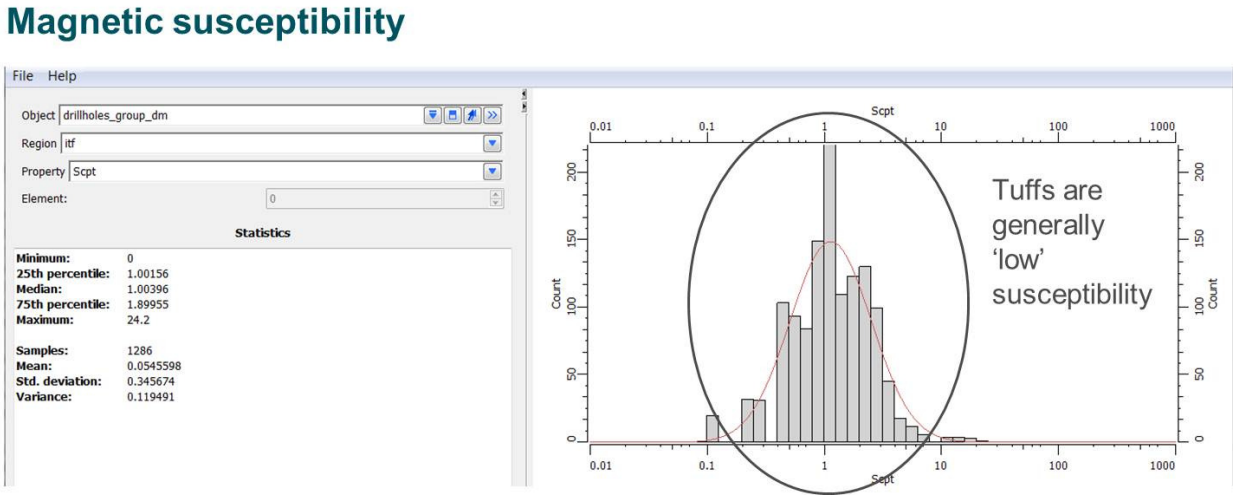

Figure 31. Summary statistics and histograms summarizing magnetic susceptibility data collected from tuff in drillcore.

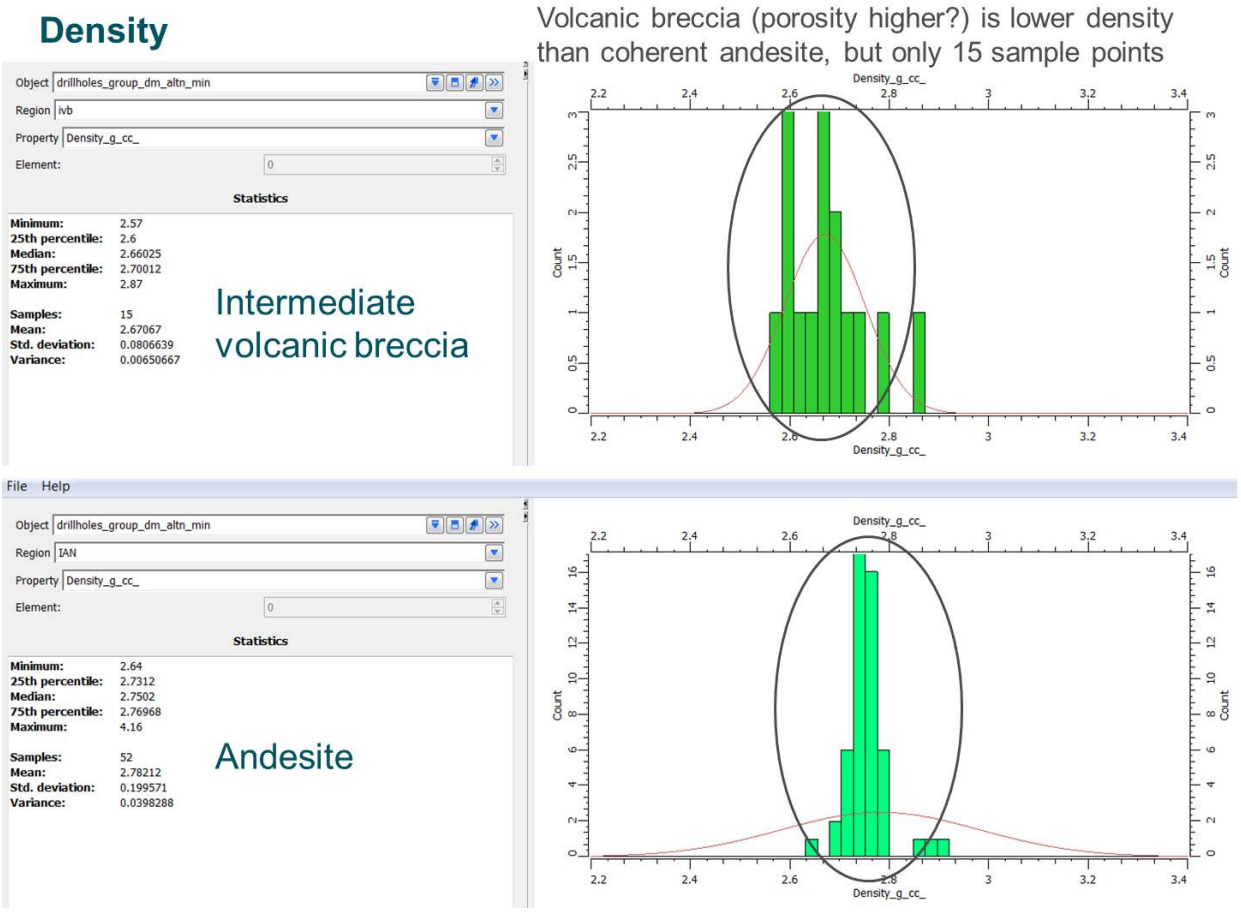

Figure 32. Summary statistics and histograms summarizing density data collected from intermediate volcanic rock samples.

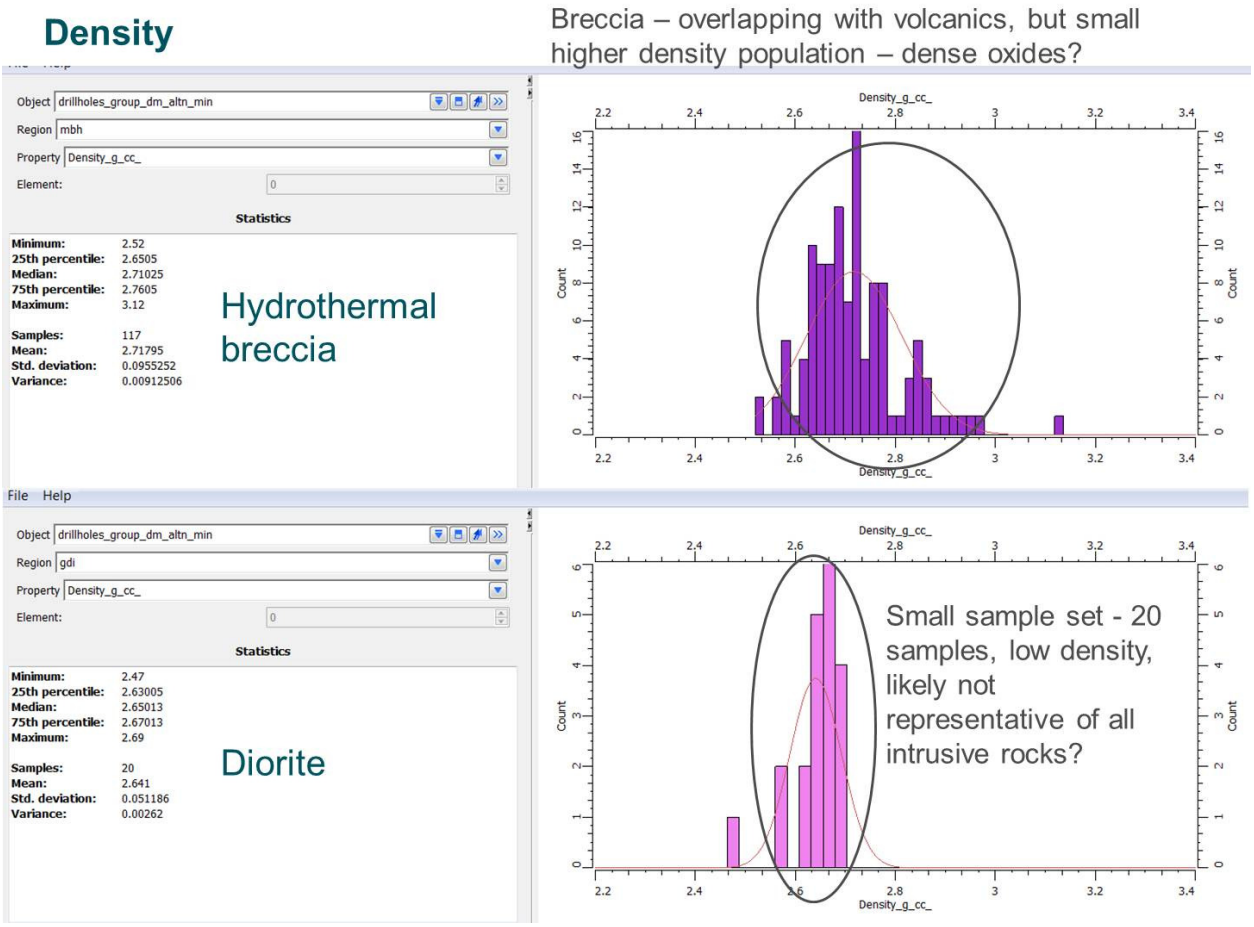

Figure 33. Summary statistics, and histograms summarizing density data collected from hydrothermal breccia and diorite intrusive rocks.

Mira Geoscience
...modelling the earth

Appendix 2. Contribution of criteria to mineral potential index value

Contributing criteria - Model 1	Target									
	1	2	3	4	5	6	7	8	9	10
(red = strong influence = (WxS)/∑W >=0.1)										
(orange = weak to moderate influence = (WxS)/∑W <0.1)										
Breccia intervals										
Proximity to magmatic-hydrothermal breccia	0.198	0.198	0.198		0.198		0.049			
Proximity to tectonic breccia			0.198							
Structure										
Proximity to NE trending faults/structures	0.099	0.198	0.049	0.198		0.198	0.198	0.198	0.198	
Proximity to NW and N trending faults/structures	0.123	0.123	0.123	0.123		0.247	0.247	0.247		0.062
Proximity to fault intersections	0.062						0.185	0.247	0.185	
MMI Geochem										
Anomalous metals from MMI - Ag	0.074	0.025	0.025					0.074	0.025	
Anomalous metals from MMI - As	0.025	0.025					0.074	0.025	0.074	
Anomalous metals from MMI - Au	0.074	0.025	0.025	0.025			0.025		0.074	0.025
Alteration indicator from MMI - Ba	0.012	0.012		0.012						
Anomalous metals from MMI - Cd	0.012	0.012					0.012		0.025	
Anomalous metals from MMI - Co	0.025	0.000	0.025	0.025			0.074	0.074	0.074	0.025
Anomalous metals from MMI - Cu	0.074	0.025	0.025	0.025			0.074	0.025	0.025	0.025
Alteration indicator from MMI - K	0.037	0.012					0.037	0.037	0.037	
Alteration indicator from MMI - Mn	0.012						0.012	0.012	0.012	0.012
Alteration indicator from MMI - P	0.012	0.012		0.012			0.037	0.012	0.012	
Anomalous metals from MMI - Zn	0.037	0.012	0.012				0.012		0.012	
Downhole Geochem										
Anomalous metals from ICP-MS - As	0.099	0.025	0.099		0.074					0.099
Anomalous metals from ICP-MS - Au	0.111	0.111	0.148		0.148					0.148
Anomalous metals from ICP-MS - Co	0.099	0.074	0.099		0.099					0.099
Anomalous metals from ICP-MS - Cu	0.148		0.148		0.111		0.037			0.148
Anomalous metals from ICP-MS - Fe	0.148				0.148					
Downhole Minerals										
Alteration indicator - presence of biotite		0.148	0.148		0.148					
Mineralization - presence of chalcopyrite	0.198	0.198	0.198		0.198					0.198
Alteration indicator - presence of Fe-oxides	0.148	0.148	0.148		0.148		0.037			0.148
Alteration indicator - presence of K-feldspar	0.148	0.111	0.148		0.148					0.148
Mineralization - presence of pyrite	0.099	0.099	0.099		0.099		0.025			0.099
Geophysics										
High magnetic susceptibility	0.247	0.247		0.247		0.247			0.247	
High conductivity		0.247		0.247	0.247	0.247	0.247			
High density	0.247	0.247		0.247		0.247		0.247	0.247	
Mineral Potential Index Value for Target	2.5679	2.3333	1.9136	1.1605	1.7654	1.1852	1.3827	1.1975	1.2469	1.2346
X	388325	388650	384750	384750	382700	388500	388825	388700	385400	383375
Y	7020050	7017250	7017825	7017825	7016375	7016300	7018650	7021375	7015900	7016925
Z	1125	975	1250	1250	1125	875	1325	1150	1150	1250

Table 9. Criteria contributing to Model 1 top 10 target centroids

Contributing criteria - Model 2	Target									
	1	2	3	4	5	6	7	8	9	10
(red = strong influence = (WxS)/∑W >=0.15)										
(orange = weak to moderate influence = (WxS)/∑W <0.15)										
Breccia intervals										
Proximity to magmatic-hydrothermal breccia										
Proximity to tectonic breccia										
Structure										
Proximity to NE trending faults/structures	0.356	0.356	0.267	0.356	0.267	0.356	0.356	0.356	0.356	0.356
Proximity to NW and N trending faults/structures	0.444	0.222	0.444	0.444				0.444		0.222
Proximity to fault intersections	0.444		0.333		0.111		0.333	0.444	0.444	
MMI Geochem										
Anomalous metals from MMI - Ag	0.133		0.044				0.044		0.044	0.044
Anomalous metals from MMI - As							0.133	0.178	0.044	0.044
Anomalous metals from MMI - Au	0.133	0.044					0.133	0.133	0.044	0.044
Alteration indicator from MMI - Ba	0.067	0.022						0.022	0.022	0.022
Anomalous metals from MMI - Cd	0.044						0.044	0.022	0.022	0.022
Anomalous metals from MMI - Co		0.044	0.044				0.133	0.133		0.044
Anomalous metals from MMI - Cu	0.133	0.044					0.044	0.133	0.044	0.044
Alteration indicator from MMI - K	0.067		0.022				0.067	0.067		0.022
Alteration indicator from MMI - Mn	0.044		0.022				0.022	0.044		
Alteration indicator from MMI - P		0.022	0.022				0.022	0.067		0.022
Anomalous metals from MMI - Zn			0.022				0.022	0.022	0.022	0.022
Downhole Geochem										
dist_to_dh_As_ppm_grtr_than_15_out_score										
dist_to_dh_Au_ppm_grtr_than_0p037_out_score										
dist_to_dh_Co_ppm_grtr_than_119_out_score										
dist_to_dh_Cu_pc_grtr_than_0p1_out_score										
dist_to_dh_Fe_pc_grtr_than_11_out_score										
Downhole Minerals										
Anomalous metals from ICP-MS - As										
Anomalous metals from ICP-MS - Au										
Anomalous metals from ICP-MS - Co										
Anomalous metals from ICP-MS - Cu										
Anomalous metals from ICP-MS - Fe										
Geophysics										
High magnetic susceptibility	0.444	0.444		0.444	0.444	0.444	0.444		0.444	0.444
High conductivity	0.444	0.444	0.444	0.444	0.444	0.444			0.444	0.444
High density		0.444	0.444	0.444	0.444	0.444	0.444			0.444
Mineral Potential Index Value for Target	2.756	2.089	2.111	2.133	1.711	1.689	2.244	2.067	1.933	2.244
X	387100	384675	388600	388550	385675	385950	385375	388775	386675	388650
Y	7020400	7016125	7021500	7016250	7016725	7016400	7015900	7018475	7018675	7017300
Z	1100	1000	1125	875	800	650	1150	1300	950	1000

Table 10. Criteria contributing to Model 2 top 10 target centroids

Contributing criteria - Model 3	Target									
	1	2	3	4	5	6	7	8	9	10
(red = strong influence = (WxS)/∑W >=0.2)										
(orange = weak to moderate influence = (WxS)/∑W <0.2)										
Breccia intervals										
Proximity to magmatic-hydrothermal breccia										
Proximity to tectonic breccia										
Structure										
Proximity to NE trending faults/structures	0.414	0.552	0.414	0.552	0.552	0.414	0.552	0.552	0.552	0.276
Proximity to NW and N trending faults/structures	0.690	0.690		0.517	0.690	0.690		0.690		0.172
Proximity to fault intersections	0.172	0.690	0.172			0.517	0.690	0.517	0.690	
MMI Geochem										
Anomalous metals from MMI - Ag										
Anomalous metals from MMI - As										
Anomalous metals from MMI - Au										
Alteration indicator from MMI - Ba										
Anomalous metals from MMI - Cd										
Anomalous metals from MMI - Co										
Anomalous metals from MMI - Cu										
Alteration indicator from MMI - K										
Alteration indicator from MMI - Mn										
Alteration indicator from MMI - P										
Anomalous metals from MMI - Zn										
Downhole Geochem										
Anomalous metals from ICP-MS - As										
Anomalous metals from ICP-MS - Au										
Anomalous metals from ICP-MS - Co										
Anomalous metals from ICP-MS - Cu										
Anomalous metals from ICP-MS - Fe										
Downhole Minerals										
Alteration indicator - presence of biotite										
Mineralization - presence of chalcopyrite										
Alteration indicator - presence of Fe-oxides										
Alteration indicator - presence of K-feldspar										
Mineralization - presence of pyrite										
Geophysics										
High magnetic susceptibility	0.690	0.690	0.690	0.690	0.690		0.690	0.690	0.690	0.690
High conductivity	0.690	0.690	0.690	0.690	0.690	0.690	0.690			0.690
High density	0.690		0.690	0.690	0.690	0.690		0.690	0.690	0.690
Mineral Potential Index Value for Target	3.34483	3.31034	2.65517	3.13793	3.31034	3	2.62069	3.13793	2.62069	2.51724
X	387925	387925	385750	384575	388475	388600	386700	388800	385150	385350
Y	7019175	7019850	7016875	7016150	7016275	7021550	7018575	7018650	7015300	7016600
Z	575	1000	825	875	875	1100	925	350	975	725

Table 11. Criteria contributing to Model 3 top 10 target centroids.